



**HAL**  
open science

## Clays and carbon nanotubes as hybrid nanofillers in thermoplastic-based nanocomposites – A review

Olawale Monsur Sanusi, Abdelkibir Benelfellah, Nourredine Aït Hocine

### ► To cite this version:

Olawale Monsur Sanusi, Abdelkibir Benelfellah, Nourredine Aït Hocine. Clays and carbon nanotubes as hybrid nanofillers in thermoplastic-based nanocomposites – A review. *Applied Clay Science*, 2020, 185, pp.105408. 10.1016/j.clay.2019.105408 . hal-03605254

**HAL Id: hal-03605254**

**<https://hal.science/hal-03605254>**

Submitted on 21 Jul 2022

**HAL** is a multi-disciplinary open access archive for the deposit and dissemination of scientific research documents, whether they are published or not. The documents may come from teaching and research institutions in France or abroad, or from public or private research centers.

L'archive ouverte pluridisciplinaire **HAL**, est destinée au dépôt et à la diffusion de documents scientifiques de niveau recherche, publiés ou non, émanant des établissements d'enseignement et de recherche français ou étrangers, des laboratoires publics ou privés.



Distributed under a Creative Commons Attribution - NonCommercial 4.0 International License

1 **Clays and carbon nanotubes as hybrid nanofillers in thermoplastic-based**  
2 **nanocomposites – A review**

3 **Olawale Monsur Sanusi<sup>a,\*</sup>, Abdelkibir Benelfellah<sup>a,b</sup>, Nourredine Aït Hocine<sup>a,\*</sup>**

4 <sup>a</sup> *INSA CVL, Univ. Tours, Univ. Orléans, LaMé, 3 rue de la Chocolaterie, BP 3410, 41034*  
5 *Blois Cedex, France*

6 <sup>b</sup> *DRII, IPSA, 94200 IVRY-SUR-SEINE, France*

7  
8 \*Corresponding author.

9 *Email addresses:* [olawale.sanusi@insa-cvl.fr](mailto:olawale.sanusi@insa-cvl.fr) (O. M. Sanusi), [nourredine.aithocine@insa-](mailto:nourredine.aithocine@insa-cvl.fr)  
10 [cvl.fr](mailto:cvl.fr) (N. Aït Hocine).

11

12

13

14

15

16

17

18

19

20

21

22 A B S T R A C T

23 Components such sensors, aerospace, heat exchanger, armour, storage, automobile and other  
24 electronics devices are continuously subjected to fluctuating thermal and mechanical stresses  
25 which consequently affect their performance, reliability and lifespan. Aerospace industry, for  
26 instance, is also in constant quest for weight reduction to attain fuel efficiency in terms of  
27 cost. It is because of these factors that engineering polymers are gaining research prominence  
28 in heat management systems, where simultaneous high strength and thermal property with  
29 significant low weight are crucial. Meanwhile, montmorillonite and carbon nanotubes are  
30 mostly used as reinforcing particles to improve physico-chemical, mechanical and thermal  
31 properties of thermoplastic matrices. This review discusses the thermoplastics-based  
32 nanocomposites reinforced with the hybrid of montmorillonite and carbon nanotubes, for  
33 high-performance applications. Influence of the nanoclay on carbon nanotube dispersion and  
34 vice versa were revealed and discussed, while used duo as hybrid in thermoplastic matrices.  
35 Consequent interaction of the hybrid nanoparticles within the host matrix influences the bulk  
36 properties of nanocomposite: Rheology, morphology, thermal stability, flame retardancy,  
37 electrical, mechanical as well as tribology. The hybrid nanofillers synergy favours efficient  
38 dispersion without destroying nanoparticles structures, leading to optimized percolation  
39 threshold and better properties of the ternary nanocomposites. Prominently, the dependency  
40 of bulk properties on nanocomposite morphological characteristics is recognised.

41 *Keywords:* Montmorillonite; thermoplastic; hybrid nanocomposite; synergy; morphology;  
42 high-performance

43

44

## 45 **1. Introduction**

46 As at year 2013, engineering plastics has already recorded a market share of more than  
47 19.6 million-metric-ton and forecasted to hit more than 29 million-metric-ton by 2020 (Das et  
48 al., 2018). Three decades back, (McCrum et al., 1988) gave two reasons for the unending and  
49 the continuous expansion to the use of polymers in Engineering: their robust properties  
50 (lightness, toughness, chemical and corrosion resistance); and versatility combined with the  
51 speed of shaping operations (Arrigo et al., 2018; Nayak, 2019) at which the raw polymers  
52 (and other additives) are transformed to functional hardware products. This is currently  
53 witnessed in terms of their applications in aerospace (Kausar et al., 2017; Pitchan et al.,  
54 2017), packaging, automobile (Shirvanimoghaddam et al., 2018), defence (Kurahatti et al.,  
55 2010; Liu et al., 2016; Venkategowda et al., 2018), anti-corrosion (Kumar et al., 2018),  
56 marine, sports, vibration control (Geng et al., 2012), piezoelectric sensor (Hosseini and  
57 Yousefi, 2017a) and numerous thermomechanical applications (Shabanian et al., 2016; Yuan  
58 et al., 2018).

59 Polymeric nanoparticle-filled composites are currently receiving tremendous attention as  
60 they are promising engineering materials with varying properties enhancement courtesy of  
61 the various nanoparticles incorporated into the polymer matrix (Mohammed, 2014; Cicco et  
62 al., 2017; Klonos and Pissis, 2017; Yuan et al., 2018; Nayak, 2019). The nanoscale particles  
63 have exceptional high aspect ratio (surface to volume ratio) that provides the needed  
64 engineering features required from polymeric composites (Yue et al., 2014; Klonos and  
65 Pissis, 2017). The properties impacted on polymers by these nanofillers focus directly on  
66 strengthening mechanical, electrical, optical and thermal behaviours as well as barrier  
67 features to temperature and fluids (Marquis et al., 2011; Yuan et al., 2017; Kumar et al.,  
68 2018). For few decades back, nanofillers include diatomite, carbon black and pyrogenic silica  
69 have been used in polymers as additives without understanding their real influence (Marquis

70 et al., 2011). However, the work of (Usuki et al., 1993) from Toyota Research and  
71 Development Group brought limelight and definite roles of nanoclays (typical nanofiller) in  
72 polymeric polyamide-6 matrix. Multi-walled carbon nanotubes (CNT), graphene (G),  
73 graphene oxide (GO), carbon nanoribbon, nanoclays including halloysite nanotubes (Chiu,  
74 2016, 2017a; Raee and Kaffashi, 2018; Ren et al., 2018; Zhu et al., 2018; Aguzzi et al.,  
75 2019), make the recent list of commonly used nanofillers (Marquis et al., 2011; Nayak,  
76 2019).

77 Therefore, researchers and industries are in constant quest of designing cost-effective,  
78 multipurpose and robust nanocomposite system for advanced material applications, especially  
79 the primary thermomechanical systems: aerospace, automobile, sensors, conductors,  
80 petroleum processing facilities (Kausar et al., 2017). For instance, aircraft industry requires  
81 low weight nanocomposites for fuel efficiency without jeopardizing strength, stiffness,  
82 thermal conductivity, impact and corrosion resistance as the system is continuously exposed  
83 to fluctuating harsh environment (Anbusagar et al., 2018). Moreover, polymer applications in  
84 modern thermal and high energy-related fields (electronics, storage and energy transportation,  
85 medicines) emphasis great attention to fire safety. This is a subset of heat management that is  
86 crucial in improving/securing the service life of a system as well as reduction of hazards by  
87 quick transfer of generated heat, which ensures maintenance of practically low temperature  
88 on the course of operational service (Chen et al., 2016; Xiao et al., 2016).

89 Nanoclay, a two-dimensional (2D) nanofiller, has been fused into polymer matrices with  
90 due mechanical, barrier and fire retardancy properties improvement. Clay platelet structure  
91 affords it the formation of protective barrier, once high degree of exfoliation with good  
92 dispersion is attained, leading to improved polymer physical performances. At this condition,  
93 low loading of clay is required. Clay's high rich intercalation chemistry affords it easy  
94 chemical modification and compatibility with polymers. Besides, it can be gotten

95 uncontaminated as mineral with little cost (Santangelo et al., 2011). Similarly, one-  
96 dimensional (1D) carbon nanotubes (CNT) continues to impact an exceedingly high electrical  
97 (Fang et al., 2019), flame retardancy (Lee et al., 2019), mechanical and thermal properties  
98 when incorporated in polymers (Khan et al., 2018; Abidin et al., 2019). The superior aspect  
99 ratio, lightweight and thermal conductivity of 2000-6000 Wm<sup>-1</sup>K<sup>-1</sup> (Cao et al., 2019) give  
100 CNT its uniqueness.

101 In an attempt towards achieving the polymeric nanocomposite high-performance goal,  
102 hybrid/combination of these two dissimilar but distinctive nanofillers is being introduced into  
103 polymer matrix to produce ternary nanocomposites. Optimal electrical and thermal  
104 conductivities, lowered flammability, high barrier system, corrosion inhibition while  
105 improving the mechanical properties are targeted (Kumar et al., 2018; Zhou et al., 2018).  
106 Hence, the review provides up-to-date information on high-performance nanocomposites  
107 developed strictly with incorporation of hybrid of montmorillonite (nanoclay) and carbon  
108 nanotubes in thermoplastic matrices. The influence of the nanoclay on carbon nanotubes and  
109 vice versa was discussed. Consequent interaction of the hybrid nanoparticles in  
110 nanocomposite was analysed on each of the bulk properties of the nanocomposite such as  
111 rheology, morphology, thermal and flame retardancy, electrical and mechanical properties.  
112 Finally, a summary of the review and other perspectives were presented.

## 113 **2. The need for hybrid of nanofillers**

114 Nanofiller roles in the mitigation of the deficiencies of polymers give rise to more novel  
115 academia researches and subsequent progressive industrial demands for the composite of  
116 thermoplastics, thermosets and elastomers (Marquis et al., 2011; Arrigo et al., 2018;  
117 Boumbimba et al., 2018; Aydođan and Usta, 2019). A little percent of nanofillers  
118 significantly changes the physicochemical, thermal, mechanical, optical, magnetic and

119 electrical properties of the hosting matrix (Papageorgiou et al., 2017a; López-Barroso et al.,  
120 2018).

121 Sizable number of researchers (Bray et al., 2013; Moghri et al., 2015; Kim et al., 2015;  
122 Bischoff et al., 2017; Ramazanov et al., 2018; Yuan et al., 2018; Radmanesh et al., 2019)  
123 have worked on the benefits of incorporating a single nanoparticle type into selected  
124 polymeric matrix (homopolymer, copolymers or mixed polymers), especially in the areas of  
125 attaining well dispersed nanofillers for toughening or improving polymeric nanocomposite.  
126 However, efficient and effective dispersion without agglomeration of the nanofillers in a  
127 polymer remains a challenge (Papageorgiou et al., 2017a; Pitchan et al., 2017; López-Barroso  
128 et al., 2018). Another impediment is the incompatibility of the constituent materials  
129 (Prashantha et al., 2014).

130 Meanwhile, nanocomposites property enhancement is directly related to the interfacial  
131 bonding formation that exists between the reinforcement phase and the matrix  
132 (Shirvanimoghaddam et al., 2017). Researchers in their varying efforts of proffering solutions  
133 resorted to the use of chemicals (either to modify the filler or as dispersing agent) (Navidfar  
134 et al., 2017), which are usually expensive, environmentally demeaning and sometime  
135 detrimental to the structure and surface of the nanofiller and/or lowering the properties  
136 expected from the bulk nanocomposite (Marquis et al., 2011; Tjong, 2014; Szeluga et al.,  
137 2015; Punetha et al., 2017). Other means of realizing an efficient dispersion is through high  
138 shear rate, which de-agglomerates the clustered nanofiller particles, and prevents further  
139 agglomeration resulted from van der Waals forces of interaction. However, high shear can  
140 cause breakage of some CNT or nanofibres particles (Levchenko et al., 2011). Moreover,  
141 conductive polymer composite (CPC) is gaining high relevance in the electromagnetic  
142 interference (EMI) shielding and carbon-material reinforced CPC is popular in this field. EMI  
143 is usually protected by reflection and absorption processes. However, single carbon-

144 reinforced CPC releases secondary EMI pollution because, in this case, the conductivity  
145 stems from reflection (Zhao et al., 2018).

146 Hybridization of nanofillers in a matrix provides safe and effective means of ensuring  
147 dispersability of certain nanofiller using other nanofiller (Levchenko et al., 2011; Szeluga et  
148 al., 2015; Papageorgiou et al., 2017a). Combination of nanofillers could bring about  
149 synergistic effects between nanoparticles (Nurul and Mariatti, 2013), offset deficiency in any  
150 of the fillers as well as improving and/or aiding dispersion and interaction of the fillers within  
151 the polymeric matrix (Safdari and Al-Haik, 2013; Papageorgiou et al., 2017a). Ultimately,  
152 benefits of the constituents' fillers are brought together in creating advanced, cost-effective  
153 (Pandey et al., 2014; Szeluga et al., 2015) and innovative materials.

#### 154 *2.1. Hybrid fillers in ternary nanocomposites*

155 Hybrid nanocomposite is a system of material that involves the combination of two or  
156 more different nanofillers in a single or multiphase polymer matrix with the purpose of  
157 achieving better material properties. Hybrid nanocomposite is pivoted on three rules: (1)  
158 economic effect by which expensive nanofiller can be combined with less expensive filler;  
159 (2) achieving a combined functional and properties enhancement; and (3) efficient  
160 preparation method (hybrid effect) (Jaafar, 2017).

161 Researchers used various combinations of fillers in different polymer matrices to achieve  
162 properties improvements. Zhao et al. (2018) used both 7 wt% (CNT and Nickel (Ni)) and 13  
163 wt% (graphene (G) and Ni) in enhancing heat dissipation for electromagnetic shield. Zhou et  
164 al. (2018) recorded over 126% enhancement in thermal conductivity on incorporating 20 wt%  
165 of GO and CNT in poly (methyl methacrylate) (PMMA). Edenharter et al. (2016) used a total  
166 of 5.5 wt% (GO and layered double hydroxide (LDH)) to realize 47% reduction in peak of  
167 heat release rate (PHRR). Xiao et al. (2016) attained 602% in thermal enhancement at hybrid



168 filler load of 22 wt% (G and CNT). With optimum combined nanofillers (ZnO and CNT) of  
169 40.5 wt% in poly (butyl methacrylate), Han et al. (2016) reported high thermal stability of the  
170 ternary composite with improved tensile strength (42%), elastic modulus (19%) and hardness.  
171 Shao et al. (2016) also employed 8.4 wt% (boron nitride (BN) and G) in achieving 350%  
172 thermal conductivity improvement. Oliveira et al. (2016) used polyetherimide and CNT  
173 doped with sodium alanate (NaAlH<sub>4</sub>) for hydrogen storage.

174 Sa et al. (2018) added only 0.8 wt% of CNT and G; and Chatterjee et al. (2012) used 0.5  
175 wt% of G and CNT nanofillers to achieve prime mechanical property. Kumar et al. (2010)  
176 reported an enhanced thermomechanical properties with just 0.5 wt% of CNT and G. Yang et  
177 al. (2011) developed CNT/G/epoxy nanocomposite filled with hybrid of 0.9 wt% G and 0.1 wt%  
178 CNT. They reported improvement of 35.4, 27 and 146% in tensile strength, Young modulus and  
179 thermal conductivity, respectively. Prasad et al. (2009) used 0.6 wt% total loading CNT and  
180 nanodiamond in achieving more than 400% stiffness and hardness boost.

181 From these cited works, carbon-based nanofillers, most especially carbon nanotubes, seem  
182 to be consistently used in polymer nanocomposite. CNT is unequal in impacting high  
183 mechanical, electrical and thermal properties in polymers (El Rhazi et al., 2018; Li et al.,  
184 2018), at comparatively low loading, due to its high aspect ratio leading to its unique capacity  
185 in formation of interconnectivity. Yet, combination of nanomaterials at high loading (7-47  
186 wt%), which might favour some features (e.g. electromagnetic shielding and flame retarding)  
187 (Pan et al., 2014), significantly hamper mechanical properties, processability and hike cost  
188 (Alshammari and Wilkinson, 2016; Edenharter et al., 2016).

189 Again, all the excellent features of CNT are worthless in isolation because the high aspect  
190 ratio and inter-tubular van der Waals forces keep the CNT nanoparticles together as large  
191 clusters (Punetha et al., 2017). Secondly, the solubility of CNT in most organic solvents is  
192 exceptionally challenging (Vyas and Chandra, 2018). Szeluga et al. (2015) emphatically

193 stated in their review that the main problem with CNT is cost and quantity of production for  
194 industrial applications. This is in agreement with (Roes et al., 2007; Almasri et al., 2018).  
195 Other effective carbon-based nanofillers, like graphene and graphene oxide (GO), have  
196 similar associated challenges (Punetha et al., 2017). These are some of the reasons that  
197 prompted and necessitated the research for hybridizing CNT with other nanofillers.

198 Similar to carbon-based nanofiller, application of small amount of layered clay, like  
199 montmorillonite (Mt), gives superior properties impact than larger percent of traditional  
200 fillers (e.g. glass fibre, calcium carbonate) (Aït Hocine et al., 2008; Prashantha et al., 2014;  
201 Raji et al., 2018) in the enhancement of the hosting matrix (Raji et al., 2016; Rahmaoui et al.,  
202 2017). Low loading of clay nanofiller attracts improved barrier performance, easier  
203 processability and provide excellent surface appearance (Prashantha et al., 2014). Shabanian  
204 et al. (2016) combined Mt and hydrogel in achieving high thermal and mechanical properties  
205 simultaneously. Clay has also been effectively used in enhancing tribological property  
206 (Golgoon et al., 2015; Azam and Samad, 2018a; Wani et al., 2018). Kausar (2016) used  
207 combination of nanogold (Au) and Mt to reinforce polyamide in developing flame retardant  
208 composite. There are reports on non-conducting nanoclays aiding CNT's dispersion and  
209 assisting in creating volume exclusion (conductive nanoparticles free zone) inside polymeric  
210 matrix and consequently led to a reduced percolation threshold (Liu and Grunlan, 2007; Wu  
211 et al., 2012; Al-Saleh, 2017; Paszkiewicz et al., 2017). More importantly, apart from being  
212 the most reported nanofiller, nanoclay is economically and industrially viable for use as nano-  
213 reinforcement in polymeric matrices (Ahamed et al., 2016; Surendran et al., 2018).

214

215

216

217 2.2. Carbon nanotube and nanoclay

218 2.2.1. Structure and properties of carbon nanotubes

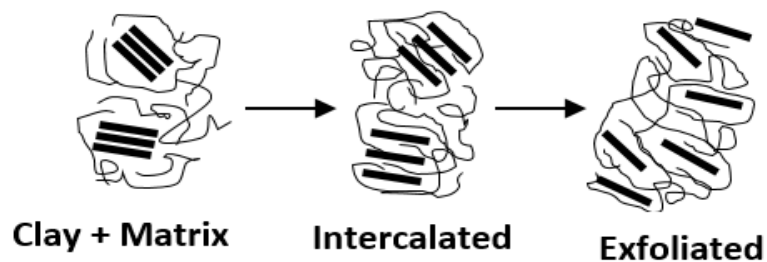
219 Carbon nanotubes (CNT) exhibit unique mechanical, thermal, electric conductivity,  
220 electromagnetic interference properties (Zhang et al., 2018) that are impacted onto its hosting  
221 polymer matrix. CNT has a ring structure featuring strong bond that is made up of C-C  
222 covalent type. This gives CNT its exceptional physical properties but resulted into low  
223 affinity to chemical reactions that makes it difficult to interact with other nanofillers as well  
224 as polymer matrix molecules (Punetha et al., 2017). Consequently, CNT most often requires  
225 surface modifications in enhancing its physicochemical interactions with other molecules and  
226 improve its processability (Shirvanimoghaddam et al., 2017). High interfacial relations within  
227 polymer nanocomposite brings about effective stress transfer to improve physical, thermal,  
228 mechanical, electrical or multifunctional features (Papageorgiou et al., 2017b; Avilés et al.,  
229 2018). There are two forms of functionalization, covalent and non-covalent, to get better  
230 orientation and improved bonding with matrix (Shirvanimoghaddam et al., 2017, 2018). CNT  
231 are available as single, double and multi-walled carbon nanotubes obtained through rolling up  
232 of a single or multiple of graphene along its axis. CNT can be produced by arc discharge,  
233 laser vaporization, chemical vapour deposition (Manikandan et al., 2013; Safdari and Al-  
234 haik, 2018). CNT reported in this review is strictly restricted to multi-walled nanotubes

235 2.2.2. Structure and properties of montmorillonite nanoclay

236 Generally, all nanoclays have the same structural description but are distinguished by their  
237 hydroxyl bond relations, positions and interlayer water numbers in each of the clay (Ray and  
238 Okamoto, 2003; Raji et al., 2018). They possess two outer tetrahedral ( $[\text{SiO}_4]^{4-}$ ) plates  
239 coordinated by silicon atoms and sandwiched on an inner octahedral ( $[\text{AlO}_3(\text{OH})_3]^{6-}$ ) plane,  
240 i.e., 2:1 phyllosilicate layered silicate mineral (Barick and Tripathy, 2011). For engineering

241 polymers, montmorillonite (Mt) is crucial and the most reported for polymer nanocomposite  
242 preparation because of its unique interfacial reactivity and high specific surface area (Seghar  
243 et al., 2011; Bunekar et al., 2018). Mt is a natural phyllosilicate from bentonite and has raw  
244 chemical formulae  $(\text{Na, Ca})_{0,3}(\text{Al, Mg})_2\text{Si}_4\text{O}_{10}(\text{OH})_2, n\text{H}_2\text{O}$  (Marquis et al., 2011).

245 The presence of the compensating charge cations and the polar molecule on the gallery  
246 basal planar makes the nanoclay to display the hydrophilic properties, and determines the  
247 interlayer space of an expansible clay mineral (Raji et al., 2016). The expansion of the  
248 interlayer space with respect to non-expansible clay affords better cation exchange capacity  
249 (CEC). Mt has high CEC (Almasri et al., 2018) which is an advantage over other clays. The  
250 hydrophilic nature makes clay difficult to be dispersed in polymer and the challenge is  
251 addressed through replacement of the interlayer cations by quarternized phosphonium or  
252 ammonium cations (Ray and Okamoto, 2003) and sol-gel technique (Bunekar et al., 2018). In  
253 short, the interlayer d-value needs to be enlarged in order to allow the penetration of the  
254 polymer molecules and/or other nanofiller into clay platelets (Fig. 1).



255  
256 **Fig. 1.** Three phases of layered clay in polymer matrix

### 257 2.2.3. Prepared Mt-CNT hybrid nanofiller

258 Aside physical addition of Mt and CNT into a matrix as regards to this review, the use of  
259 Mt-CNT hybrid filler, prepared by growing CNT over Mt via catalytic chemical vapour  
260 deposition (CCVD) (Fig. 2) that aids homogenous dispersion within polymer (Manikandan et  
261 al., 2013), is also cited. Details on CCVD process can be accessed in (Madaleno et al., 2012).

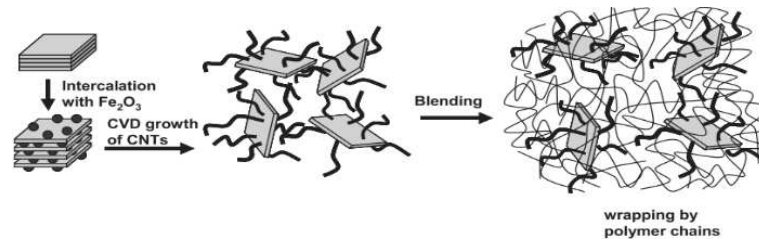


**Fig. 2.** Route of growing CNT on Mt and blending with polymer (Zhang et al., 2006)

### 3. Preparation techniques of ternary nanocomposites

Polymer nanocomposite properties are dependent on the processing technique adopted for its production and ultimately dispersion of the nano-reinforcements in terms of effective distribution and exfoliation in the matrix (Zaferani, 2018). Besides the conventional melt blending, solution blending and in-situ polymerization, electrospinning and high-energy ball-milling were recently reported. Table 1 lists the reviewed thermoplastics polymers specifically filled with hybrid of CNT and clay (Mt) for high-performance applications.

**Table 1**

Summary of thermoplastics polymer filled with hybrid of CNT and Mt.

Matrix	Optimum filler concentration (wt%)			Dispersion Technique	Focused Application	Reference
	CNT	Mt	CNT/Mt**			
ABS	1	1		Melt-mixing	Flame retardant	Ma et al. (2007)
EVA	1	3		Melt-mixing	Thermo-mechanical	Peeterbroeck et al. (2004)
EVA	2.5	2.5		Melt-mixing	Flame retardant cable	Beyer (2005)
EVA	2.5 <sup>s</sup>	2.5 <sup>s</sup>		Melt-mixing	Flame retardant cable	Beyer (2006)
Nafion			2	Solution-mixing	Fuel cell	Manikandan et al. (2012)
HDPE	1	1		Solution- and melt-mixing	Thermo-mechanical	Silva et al. (2014)
HDPE	0.6	0.4		Melt-mixing	Flame retardant	Rao et al. (2015)
UHMWPE	1.5	1.5		Solution-mixing	Tribology	Azam and Samad (2018b)
PA-6			1	Melt-mixing	Mechanical	Zhang et al. (2006)
PCL			0.5	Melt-mixing	Thermo-mechanical	Terzopoulou et al. (2016)
PET			3	Melt-mixing	Thermo-mechanical	Gorrasi et al. (2014)

PLA			3	Centrifugal ball milling	Sorptive and electrical	Santangelo et al. (2011)
PLA			3	Melt-mixing	Irradiation	Gorrasi et al. (2013)
PLA	2	10 <sup>£</sup>		Melt-mixing	Flame retardant	Hapuarachchi and Peijs (2010)
PP	NS	3		Melt-mixing	Mechanical	Olalekan et al. (2010)
PP	0.5*	0.5*		Melt-mixing	Electrical conductor	Levchenko et al. (2011)
PP	1	1		Melt-mixing	Mechanical	Prashantha et al. (2014)
PP	0.3	3		Melt-mixing	Thermal and flame retardant	Pandey et al. (2014)
PP	0.5	0.5		Melt-mixing	Electrical and thermo-mechanical	Al-Saleh (2017)
PS-b-PI-b-PS			1	Solution-mixing	Mechanical	Enotiadis et al. (2013)
PU			0.25	In-situ polymerization	Polymer foam	Madaleno et al. (2013)
PVA			3	Solution-casting	Thermo-mechanical	Zhao et al. (2009)
PVB	0.2	2		Solution-mixing	Impact resistance	Stern et al. (2018)
PVDF	1.9	3		Melt-mixing	Vibration	Geng et al. (2012)
PVDF	0.5	0.5		Melt-mixing	Electrical and thermo-mechanical	Chiu (2014)
PVDF	0.5	1		Melt-mixing	Charge storage	Khajehpour et al. (2014)
PVDF	0.05	0.1		Electrospinning	Piezoelectric	Hosseini and Yousefi (2017b)
PVDF	0.05	0.1		Electrospinning	Sensor Piezoelectric	Hosseini and Yousefi (2017a)

273 \*%volume; \$part per resin

274 <sup>£</sup>sepiolite nanoclay; NS not stated

275 \*\*Hybrid CNT/clay produced via CCVD. ABS-acrylonitrile-butadiene-styrene ; EVA-ethylene-vinyl acetate;

276 HDPE-high-density polyethylene; PA-polyamide; PP-polypropylene; PET-poly(ethylene terephthalate); PLA-

277 polylactide; PS-b-PI-b-PS-polystyrene-b-poly(isoprene)-b-polystyrene; PU-polyurethane; PVA-polyvinyl

278 alcohol; PVB-polyvinyl butyral; PVDF-polyvinylidene fluoride; PCL-poly( $\epsilon$ -caprolactone); UHMWPE-ultra-

279 high molecular weight polyethylene.

### 280 3.1. Melt-mixed nanocomposites

281 Melt mixing is a process of applying both high temperature and shear force in order to

282 prepare nanocomposites with well-dispersed nano-reinforcement. It is highly popular for

283 industrial/academic research and development as it supports various forms of polymer that

284 are not suitable for other methods. It requires no solvent/chemical, supports high volume of

285 bulk polymer and it's low cost with the least environmental issues (Bunekar et al., 2018).

286 With regards to the thermoplastics reinforced with hybrid CNT/Mt, many researchers (Zhang

287 et al., 2006; Hapuarachchi and Peijs, 2010; Olalekan et al., 2010; Levchenko et al., 2011;

288 Geng et al., 2012; Chiu, 2014; Khajepour et al., 2014; Pandey et al., 2014; Prashantha et al.,  
289 2014; Terzopoulou et al., 2016; Al-Saleh, 2017) have reported properties enhancement with  
290 melt-mixing method. Few of the works that draw substantial attention are discussed below.

291 Peeterbroeck et al. (2004) employed melt-blending approach in developing a ternary  
292 nanocomposite using CNT and organo-modified Mt in EVA. In the binary system of  
293 EVA/Mt, degradation temperature was delayed by 52°C while EVA/CNT composite had only  
294 37°C delay. On incorporating hybrid of 3 wt% Mt and 1 wt% CNT nanofillers into the EVA,  
295 56°C highest delay was reported. The flammability behaviour was also studied by comparing  
296 binary systems (each filled with 4.8 wt% Mt or CNT) and the ternary having the same  
297 combined nanofillers loading. All recorded enhanced flame retardancy but ternary  
298 EVA/CNT/Mt (CNT:clay; 2.4:2.4) recorded the highest PHRR reduction of 36% with an  
299 accompanying lessening of Mt detrimental effect on time to ignition which improved from 67  
300 s (Mt/EVA) to 71 s. The ternary supremacy was associated with formation of synergistic  
301 uniform crust by Mt/CNT over the burning composite that limited the heat and gas diffusion,  
302 and consequently lessened its flammability. Well-dispersed clay platelets, in the presence of  
303 CNTs, was reported thus aided the barrier effects.

304 Ma et al. (2007) prepared the hybrid of organoclay and CNT via melt mixing in enhancing  
305 ABS flame retardancy. In studying the influence of CNT on clay, morphological state of  
306 dispersion of the clay in the composites were analyzed, using X-ray diffraction, in both  
307 ABS/2clay (loaded with 2 wt% clay) and ABS/1clay/1CNT (1 wt% clay; 1 wt% CNT). They  
308 achieved 3.77 nm interlayer space of the clay in ternary ABS/1clay/1CNT against 3.67 and  
309 1.92 nm for binary ABS/2clay and ordinary clay particle respectively. This meant that clay in  
310 the ternary attained better exfoliation in the presence of CNT. They also assessed and  
311 compared the distribution of filler(s) in both binary and the hybrid-filled ABS. The reported  
312 transmission electron microscopy (TEM) affirmed that binary systems prepared with clay,

313 ABS/2Mt, produced composite with insignificant clay exfoliation; and ABS/2CNT with more  
314 CNT aggregations within matrix. However, the ternary system revealed CNT intercalated  
315 into the Mt interlayer spaces, which produced good interaction between the fillers and matrix  
316 structures, and CNT was able to form structured network with the clay platelets. Hence, the  
317 superiority of ternary fire retardancy over binary ones.

318 In determining the susceptibility of the residual ash to further heating, they calculated  
319 graphitization degree. Ternary ABS/1clay/1CNT reportedly produced ash with higher  
320 graphitization than ABS/2CNT, which asserted lower vulnerability of the ternary residual ash  
321 to further thermal oxidation on prolonged exposure. They also performed rheological  
322 characterizations to further probe into the establishment of 3D network structure by the  
323 hybrid fillers, with respect to the single-filled composites. In relation to both storage and loss  
324 moduli, the ABS/1clay/1CNT recorded highest values followed by ABS/2CNT and  
325 ABS/2clay, while ABS matrix had the least property. They explained the behaviour from  
326 nanomaterials' dimensional perspective that the incorporation of high aspect ratio 1D  
327 nanotube and 2D nanoclay formed an efficient confined space and created a 3D structure that  
328 restricted polymer chains movement. Consequently, enhanced the rheological and flame  
329 retardancy characteristics of hybrid-filled nanocomposite over individual nanofiller inclusion.

330 By comparing the processing behaviour of ternary CNT/clay/PP and binary CNT/PP  
331 during melt-mixing, Al-Saleh (2017) was able to substantiate reduction in the amount of CNT  
332 required for the ternary CNT/clay/PP to attain percolation threshold concentration compared  
333 to binary CNT/PP with the same 1 wt% CNT loading. Every two seconds, he monitored the  
334 mixing-torque of the nanocomposite against time. It was found that the mixing torque of the  
335 binary with only 1 wt% CNT loading was higher than that of ternary system with 1 wt% CNT  
336 and 1 wt% clay loading. He concluded that the additional incorporated clay in the ternary



337 served as plasticizers and lowered viscosity, which promoted a reduced shear on the CNT  
338 particles. Meanwhile, increase of mixing energy/torque is said to degrade CNT particles.

### 339 *3.2. Solution-mixed nanocomposites*

340 Solution mixing method gives effective nanofiller dispersion and it involves three main  
341 steps: introduction and dispersion of nanofiller(s) into a suitable solvent, mixing with the  
342 parent matrix (magnetic, heating, sonication), and drying of the material. Few challenges are  
343 inherent with this method: cost and environmental issues linked with chemicals, and the use  
344 of ultrasound in aiding polymer solution mixing that may result in reduction of polymer  
345 molar mass (Isitman and Kaynak, 2010). Zhao et al. (2009), Manikandan et al. (2012), Azam  
346 and Samad (2018b) reported high properties enhancement by adopting this approach in  
347 incorporating CNT-Mt hybrid, while Stern et al. (2018) is discoursed for its discovery.

348 Stern et al. (2018) used the hybrid of Mt and CNT to produce PVB-based nanocomposite  
349 through solution mixing. In aiding filler(s) dispersion, they applied and varied sonication  
350 power (100 W, 700 W), and then studied the effect on morphological and mechanical  
351 properties. They reported better dispersions of CNT, clay or hybrid of the fillers in PVB at  
352 higher sonication power. Fracture toughness of both hybrid and single-filled matrices  
353 affirmed this. At 700 W, ternary PVB/CNT-0.2/nanoclay-2 recorded 176% peak fracture  
354 energy improvement while PVB/CNT-0.2 and PVB/nanoclay-2 had 104 and 118%  
355 respectively. However, scanning electron microscopy (SEM) and small-angle X-ray  
356 scattering (SAXS) employed in studying the nanoclay state of exfoliation revealed a surprise.  
357 At 100 W power application, PVB/nanoclay-1wt% and PVB/CNT-0.1wt%/nanoclay-1wt%  
358 had interlayer d-values of 17.58 and 17.62 nm; while having 18.36 and 18.34 nm at 700 W  
359 sonication respectively, but both were lower than 20.31 nm of the clay particles. This implies  
360 a lack of intercalation or exfoliation of the incorporated clays despite the high fracture  
361 toughness property of the composites. After that, they found that high surface roughness

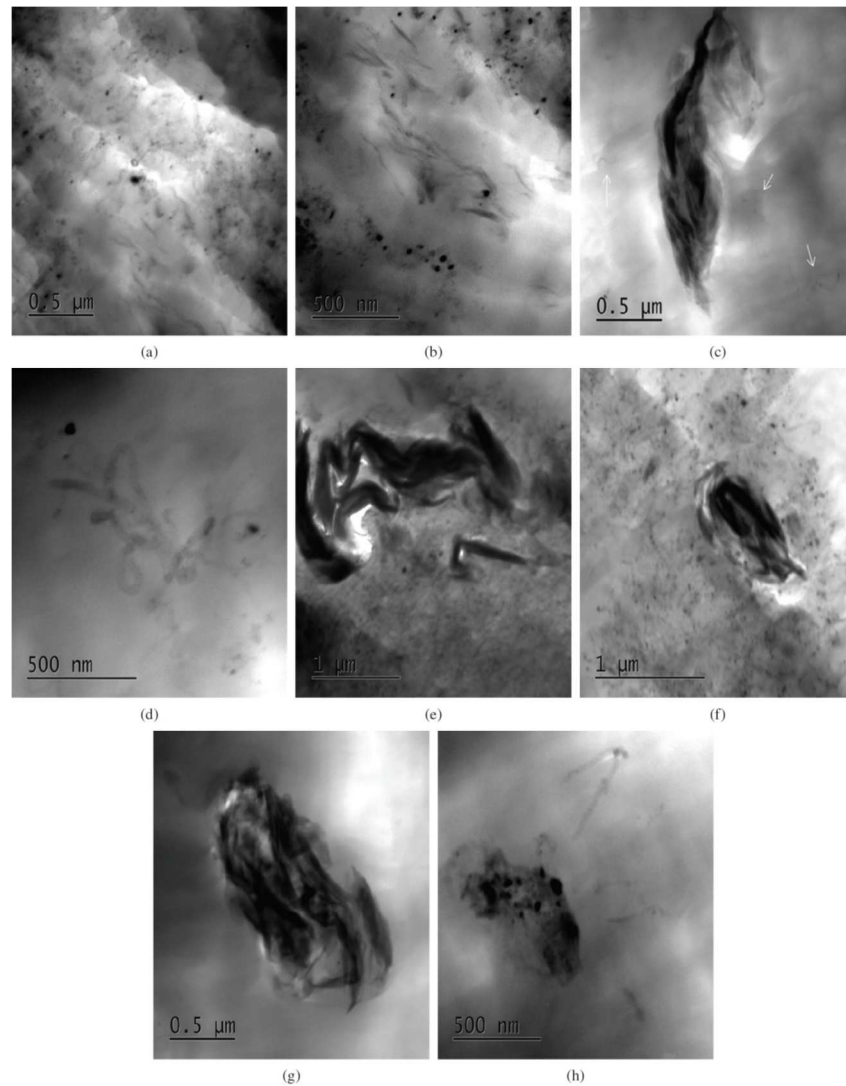
362 value of fractured ternary composite surface, caused by the hybrid fillers synergism, was  
363 responsible for the high mechanical property. Consequently, they termed surface roughness  
364 as a determinant of fracture toughness aside the famous stress transfer mechanism. Two, high  
365 sonication power generates more filler(s) particles which support improved fracture strength.

### 366 *3.3. Comparing solution-mixing and melt-mixing methods*

367 Silva et al. (2014) compared nanocomposite of HDPE using the hybrid of 1 wt% CNT (C)  
368 and 1 wt% of either natural clay (N) or organoclay (30B) by both melt-mixing (m) and  
369 solution-mixing (s) methods. The two mixing methods, to prepare binary unmodified natural  
370 clay/HDPE, reportedly caused no clay exfoliation in the matrix. Equally, modified clay  
371 reportedly remained as agglomerates in HDPE with melt-mixing but well exfoliated with  
372 solution method, owing to its organophilic character of swelling to allow HDPE matrix-clay  
373 interaction in the presence of solvent. On the contrary, melt-mixing produced better CNT  
374 dispersion in HDPE/CNT binary composite than solution method (although inefficient  
375 magnetic stirring was reported as the cause of the re-agglomeration of CNT particles). For the  
376 ternary nanocomposites by solution blending (Figs. 3a, b, e, f), irrespective of the nanoclay  
377 hybridized with CNT, the nanotubes were well dispersed but preferentially formed structure  
378 with organoclays (PE/C/30B-s) (Figs. 3a, b). However, ternary composites prepared by melt  
379 blending (Figs. 3c, d, g, h) showed agglomerates of nanoclays enclosed by dispersed CNT  
380 with some clusters.

381

382



383

384 **Fig. 3.** TEM images at different resolutions for: PE/C/30B-s (a) and (b); PE/C/30B-m (c) and  
 385 (d); PE/N/C-s (e) and (f); PE/N/C-m (g) and (h) (Silva et al., 2014)

386 The mechanical study revealed improved Young's modulus irrespective of the preparation  
 387 method or clay. Melt-mixed ternary composites got 16% peak enhancement, while binary and  
 388 ternary samples with nanoclay via solution mixing only attained 9% modulus improvement.  
 389 For hardness, ternary composite (PE/C/30B-s) prepared with organoclay through solution-  
 390 mixing recorded 28% peak enhancement but 20% for PE/C/30B-m (melt mixing). They  
 391 established the superiority of using organo-modified nanoclay over natural clay as it is more  
 392 compatible with CNT in effecting synergistic reinforcement. They explained that the solution

393 mixing offered an easier diffusion of the nanoparticles within the matrix, which contributed  
394 to homogenous dispersion of clay/CNT and making them as nucleating agents/sites for  
395 crystallization. They also restrained the polymer chains mobility, thus requiring higher load  
396 to induce plastic deformation.

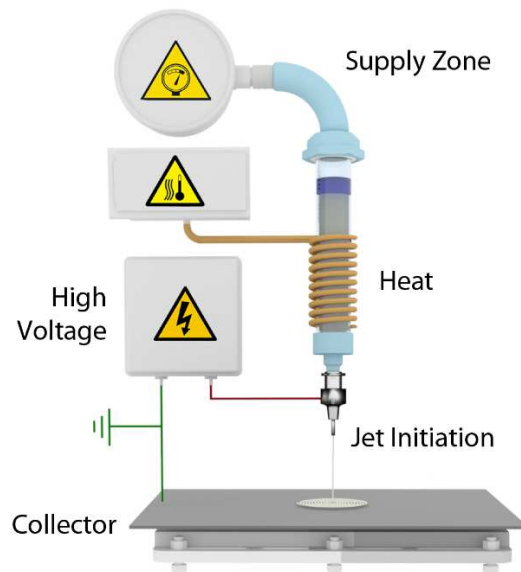
#### 397 *3.4. In-situ polymerization method*

398 Although it was adopted to prepare binary poly(ethylene terephthalate)/clay (Tsai et al.,  
399 2014), polyimide/graphene oxide (Wang et al., 2011), nylon-6/graphene (Xu and Gao, 2010),  
400 and poly(methyl methacrylate) incorporated with graphene (Potts et al., 2011), in-situ  
401 polymerization is rarely compatible with latest techniques of polymer processing (Dlamini et  
402 al., 2019) and commonly employed for low viscous matrix like liquid epoxy (Safdari and Al-  
403 haik, 2018). To the best of our review, Madaleno et al. (2013) have only applied the method  
404 for clay/CNT-filled high-performance thermoplastics polymer nanocomposite.

405 Madaleno et al. (2013) utilized Mt-CNT prepared by CCVD to develop PU nanocomposite  
406 foam with varying loading of Mt-CNT (0.25, 0.50, 1.00 wt%). They reported that hybrid  
407 fillers at lower concentrations showed no agglomeration, but higher inclusion produced more  
408 agglomerates due to the closeness of particles that are of high surface energy and area. All the  
409 composites attained improved compressive strength and thermal stability over the neat  
410 matrix. Yet, prepared Mt-CNT significantly increased degradation rate of the nanocomposite,  
411 associated with metallic particles used in exfoliating clay in CCVD process.

#### 412 *3.5 Electrospinning and high-energy ball milling methods*

413 Electrospinning method can be defined as a process of drawing continuous polymeric fibre  
414 from either a polymer solution or polymer melt, based on an electrohydrodynamics  
415 phenomenon, using electrostatic force in a liquid-jet form to fabricate polymer composite  
416 (Brown et al., 2016). Fig. 4 shows a schematic melt electrospinning system.



417

418

**Fig. 4.** Melt electrospinning system set up (Brown et al., 2016)

419

420

421

422

423

424

425

426

427

428

429

430

431

432

433

Hosseini and Yousefi (2017a, b) prepared a ternary of PVDF (A), CNT (CN) and modified clay. 0.15 wt% total fillers loading were varied (A/0.05CN/0.1clay, A/0.075CN/0.075clay and A/0.1CN/0.05clay) in studying the effects on PVDF's crystalline structure; and invariably on the piezoelectric performance of the resulting nanocomposites. They observed high level of nanofillers exfoliation in the matrix, for instance, the Mt d-value peak from the XRD disappeared in all composite formulations that connoted a high level of dispersion. They reported reduced composite fibre diameter as the quantity of clay increased (while CNT reduced), that favoured lower viscosity with reduced nanotubes tangles and formation of  $\beta$ -phase crystal, which enhanced the PVDF piezoelectric behaviour. Mt interacted with  $-\text{CH}_2$  group in the PVDF, after being stretched by the high electric field during electrospinning, leading to stabilization of targeted  $\beta$ -phase crystals and prevented its transformation to  $\alpha$ -phase.

The significant of  $\beta$ -phase content and polarization achieved was verified by piezoelectric impact sensory of neat PVDF, A/0.1CN/0.05clay, A/0.075CN/0.075clay and A/0.05CN/0.1clay composites. They recorded 8.25, 8.4, 9.03 and 10.9 mV/N sensitivities,

434 respectively. They explained that the high sensitivity of A/0.05CN/0.1clay was due to the  
435 little amount of the hybrid fillers (0.15 wt%) which was not sufficient to cause any PVDF's  
436 polar dilution and detrimental effect on its mechanical flexibility. However, the widest sound  
437 absorption by the composite was dependent on higher CNT content (A/0.1CN/0.05clay); and  
438 it recorded the least electrical resistance, signifying established network formation at very  
439 low loading.

440 Ball milling is another environmental-friendly method adopted by (Santangelo et al.,  
441 2011) to developed PLA nanocomposite using clay-CNT nanofiller produced by CCVD  
442 growth of CNT over nanoclay (muscovite). Enhanced sorptive and electrical conductivity  
443 with 6-9 orders of magnitude in nanocomposite over the pristine matrix was reported. Gorrasi  
444 and Sorrentino (2015) wrote a review on forms of mechanical milling for nanocomposite.

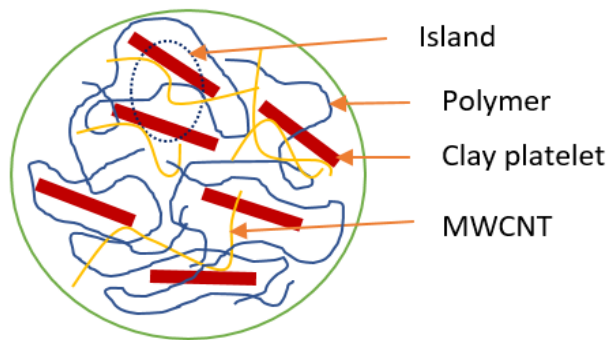
#### 445 **4. Properties of polymeric nanocomposites reinforced with hybrid of nanoclay-CNT**

##### 446 *4.1. Rheological properties*

447 Mixing torque depicts the composite viscosity variations coordinated by the instantaneous  
448 microstructural rearrangements. Rheological investigation serves as the tool to evaluate the  
449 existing network structure between matrix and the incorporated nanofiller(s) (Rueda et al.,  
450 2017; Singla et al., 2017).

451 Pandey et al. (2014) developed ternary nanocomposite comprised of polypropylene (PP),  
452 clay (C15A, 3 wt%) and CNT (0.3 wt%) by melt blending. They reported improved storage  
453 and loss moduli of all composites over neat PP, while the ternary system had the highest  
454 improvement. The same trend was reported for the viscosity of the composites but unlike  
455 storage and loss moduli that improved with frequency, viscosity reduced with frequency  
456 (non-Newtonian characteristics). The improved rheological behaviour of ternary system over  
457 the binary was attributed to the high synergetic interaction of the clay platelets and CNT.

458 CNT has a high degree of affinity for nanoclay, thereby the presence of clay lead to  
459 interruption of bundled CNT network and establishing an island of intact clay-CNT three  
460 dimensional (3D) network structures that restrain polymer chains motion (see the mechanism  
461 in Fig. 5), leading to enhanced viscosity and modulus. The formed intact network effected  
462 improved thermal and flammability property of ternary by the formation of protective char  
463 with a tight and continuous structure that prevented thermal and mass transfer.



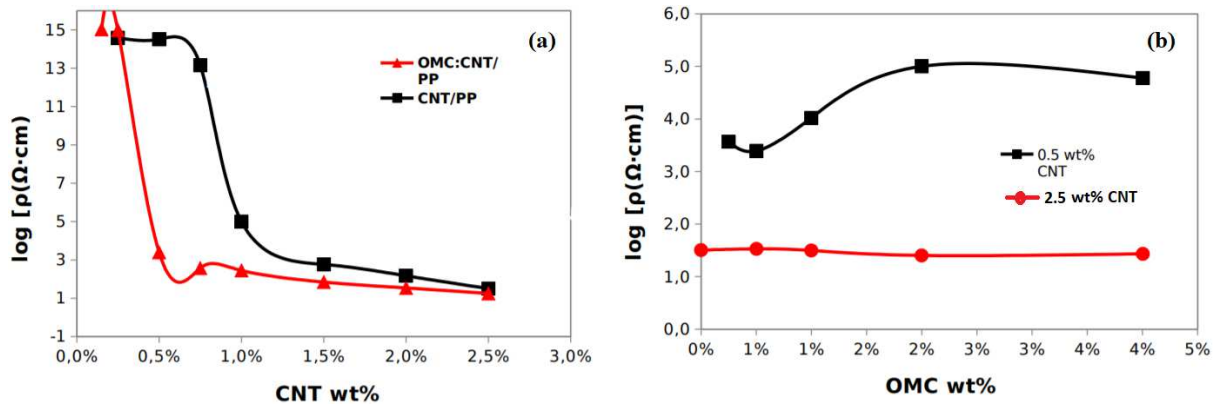
464

465 **Fig. 5.** Clay platelet-CNT interaction mechanism in ternary system

466 Al-Saleh (2017) reported 50% reduction in the quantity of CNT needed for the ternary  
467 CNT/clay/PP to attain electrical percolation threshold concentration (EPTC), compared with  
468 binary CNT/PP that required 1 wt% CNT (Fig. 6a). The researcher further probed clay  
469 influence on electrical resistivity of percolated composites, 0.5 wt% CNT/PP and 2.5 wt%  
470 CNT/PP, by adding varying amount of clay. They reported negligible effect on 2.5-CNT/PP  
471 because of an established conductive network, while clay increase beyond 0.5-synergistic  
472 EPTC upset the "young" CNT-network in 0.5-CNT/PP, with observed resistivity growth (Fig.  
473 6b). From rheological study, the researcher found that the mixing torque required by ternary  
474 with clay/CNT (having total 2 wt% hybrid fillers) was lesser than the binary composite  
475 without clay (only 1 wt% CNT), which was expected to require higher torque. Therefore, the  
476 researcher established that the clay inclusion functioned as a plasticizing agent in the matrix  
477 that facilitated viscosity and shear stress reduction thereby maintained CNT high aspect ratio,

478 influenced the composite crystallinity and improved CNT-networks formation. This resulted  
 479 in a 50% electrical percolation reduction in ternary system. Similarly, Hosseini and Yousefi  
 480 (2017b) reported higher dynamic viscosity, storage and loss moduli in electrospun  
 481 PVDF/CNT/clay ternary composite compared to neat or single-filled matrix.

482



483

484 **Fig. 6.** (a) Percolation behaviour of CNT/PP with(out) clay (OMC); (b) influence of clay on  
 485 electrical resistivity of both 0.5-CNT/PP and 2.5-CNT/PP composites (Al-Saleh, 2017)

#### 486 4.2. Morphological Properties

487 Several examinations are required for better understanding of the structure morphology,  
 488 interfacial interaction and nanofillers dispersion in a polymer matrix, like using Raman  
 489 microscopy, scanning electron microscopy (SEM), TEM, Fourier transform infrared  
 490 spectroscopy (FTIR), X-ray diffraction (XRD). It is worth noting that the morphology of a  
 491 nanocomposite dictates its overall performance (Mayeen et al., 2018).

492 Manikandan et al. (2012) utilized CCVD-prepared Mt-CNT fillers to achieve defect-free  
 493 homogenous Nafion (perfluoro-sulphnoyl-fluoride copolymer) nanocomposite for fuel cell  
 494 application. From microstructural study, strong adhesion in Mt-CNT-Nafion nanocomposite  
 495 was proven as broken CNTs particles reportedly remained stuck within matrix. The clay



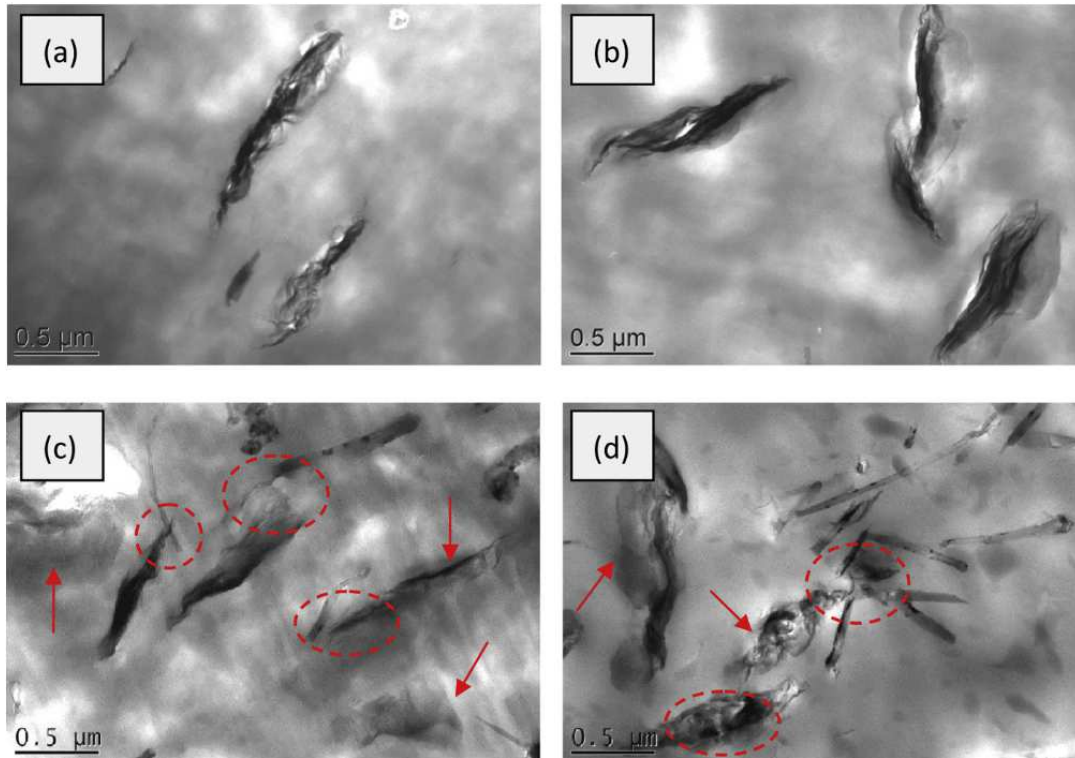
496 layered-structure favoured the uniformity of Nafion over CNT resulted in high thermal  
497 stability.

498 Chiu (2014) used the hybrid of Mt (C) and CNT (T) in developing PVDF nanocomposite  
499 using melt-mixing approach. Binary and ternary composites of varying nanofiller were  
500 prepared with the following designations: C1 (PVDF/Mt-1 wt%), T3 (PVDF/CNT-3 wt%);  
501 and CT5 (PVDF/Mt-2.5 wt%/CNT-2.5 wt%). On comparing the morphology of C1 and  
502 hybrid reinforced CT5, SEM revealed that the inclusion of CNT aided the dispersion of  
503 nanoclay in CT5; unlike Mt aggregation found in C1. Chiu related the behaviour to increase  
504 in the melt viscosity when CNT was added to binary PVDF/Mt, which led to intensive  
505 dispersion of Mt (Fig. 7). Similarly, on combining CNT with Mt, XRD diffraction angle  
506 reportedly shifted to the left and became sharpened, which indicated d-value increase and  
507 perfect crystallite size respectively. The morphological study confirmed that the addition of  
508 only Mt or the hybrid of the fillers created polymorphism in PVDF matrix. He found that low  
509 crystallization cooling rate generated high  $\beta$ -form crystals.

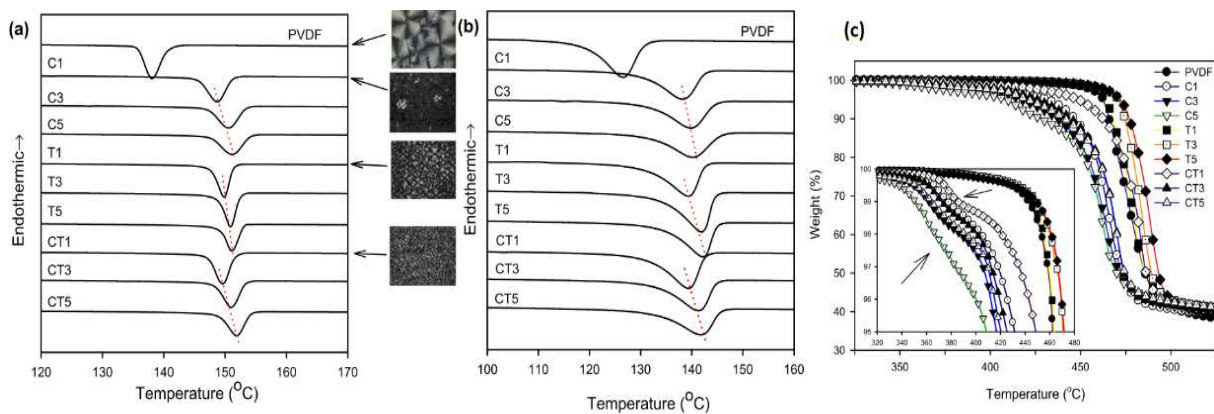
510 He also described the thermal property (DSC) of the composite from the morphological  
511 perspectives. It was observed that individual introduction of Mt or CNT and their hybrid  
512 (Mt/CNT) significantly acted as nucleating agent for the matrix crystallization which led to  
513 increase in both onset and peak crystallization temperatures (Figs. 8 a, b); and these increased  
514 with nanofiller mass fraction. Fig. 8a also includes structure of each of the composites and  
515 shows the uniformity of structure generated with the use of hybrid filler.

516 In terms of thermal stability, inclusion of CNT in the binary PVDF/CNT (T) improved the  
517 thermal degradation of the composite, which suggested good CNT dispersion and protective  
518 layer/char formation during heating. However, upsurge of Mt in PVDF matrix led to reduced  
519 degradation temperature for the PVDF/Mt (C), while ternary system PVDF/CNT/Mt (CT)  
520 displayed thermal stability that falls in between that of the improved binary PVDF/CNT and

521 the reduced binary PVDF/Mt (Fig. 8c). The reduction of thermal stability of Mt-included  
 522 composite has been related to the effect of organic modifier on Mt particles. Nonetheless,  
 523 CNT upturned the deficiency in Mt while hybridized in the ternary.



524  
 525 **Fig. 7.** TEM of PVDF composites containing (a) 1wt% Mt (b) 3 wt% Mt (c) 1.5wt% Mt/1.5  
 526 wt% CNT (d) 2.5wt% Mt/2.5wt% CNT (Chiu, 2014)



527  
 528 **Fig. 8.** (a) DSC cooling curve 15°C min<sup>-1</sup>; (b) 40°C min<sup>-1</sup> (c) TGA curves- N<sub>2</sub> of PVDF and  
 529 its composites (Chiu, 2014)

530 *4.3. Thermal and flame retardancy properties*

531 Polymer combustion cycle involves thermal decomposition that yields volatile as well as  
532 highly inflammable organic compounds, at comparatively low temperature, and emits large  
533 quantum of heat that causes further polymer degradation and accelerates growth of fire  
534 (Rothon and Hornsby, 1996; Dasari et al., 2013). Several approaches are used for protection  
535 against fire by interrupting the combustion cycle: modification of thermal degradation  
536 process, oxygen denial, or inhibition of back-flow of heat (Rothon and Hornsby, 1996; Dasari  
537 et al., 2013). Flame retardants (Dasari et al., 2013) or intumescent flame retardants (Yuan et  
538 al., 2017) are added to polymer to improve flame retardancy. However, environmental and  
539 health-related concerns, aside high loading that has a deteriorating impact on processability  
540 (Rothon and Hornsby, 1996; Bourbigot et al., 2019) and mechanical behaviour of resulting  
541 nanocomposite (Feng et al., 2018), pose a major challenge.

542 Nanomaterials present eco-friendly flame, smoke and toxicity performances at a very low  
543 loading percentage due to its high aspect ratio (Yuan et al., 2017). Few examples include  
544 layered silicates (Liu et al., 2019; Zhu et al., 2019), carbon nanotubes (Ji et al., 2018),  
545 graphene oxide (Fanga et al., 2019; Wang et al., 2019). Beyer (2005, 2006) attained about  
546 57% reduction of PHRR on incorporation of 2.5 phr each of CNT and nanoclay in poly  
547 (ethylene-vinyl acetate) copolymer. The heat release capacity was drastically reduced by 58%  
548 on incorporation of 2 wt% CNT and 10 wt% clay in PLA matrix (Hapuarachchi and Peijs,  
549 2010). Rao et al. (2015) prepared flame retardant nanocomposite of HDPE with blend of  
550 modified clay and CNT. They reported improved thermal stability in the binary system with  
551 CNT (1 wt%) over the neat HDPE; while with incorporation of only clay (1 wt%) thermal  
552 stability fell below pristine HDPE. HDPE/clay binary composite recorded 123.2 and  
553 132.16°C for its onset and peak degradation temperatures respectively, while 127.5 and  
554 135.34°C for HDPE/CNT in the same order. Meanwhile, simultaneous addition of same ratio

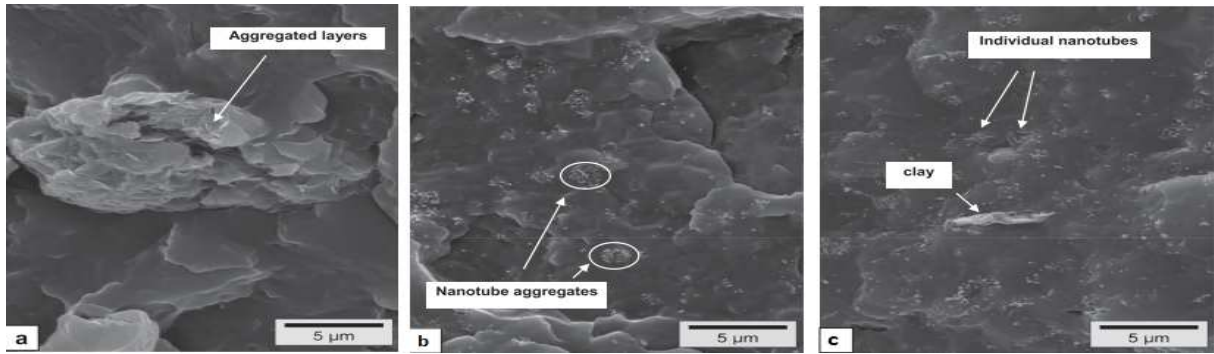
555 of CNT (0.5 wt%) and clay (0.5 wt%) in the matrix showed the best thermal properties: 12%  
556 char residue, highest delay in degradation temperatures (onset, 128.1°C; peak, 137.94°C) and  
557 the least percentage crystallization that means efficient components interaction.

558 Also, in an effort to determine the optimum ratio of CNT to clay (total loading: 1 wt%) for  
559 flammability resistance application in the ternary HDPE/CNT/clay, nanoclay was varied in  
560 0.8 - 1 wt% (i.e., CNT 0.2 - 0 wt%) and vice versa. In comparison with neat HDPE, they  
561 reported 66.8% reduction in peak heat release rate (PHRR) at optimum formulation of  
562 0.6CNT/0.4clay/HDPE. They reported that CNT migrated faster than clay to the matrix  
563 surface in forming insulating protective layer, which prevented gas or energy transport. Time  
564 to ignition was said to be favoured with CNT increase, as formed char layers served as heat  
565 sinks that deferred ignition and degradation. Ternary's mechanical property was also  
566 enhanced through enhanced interfacial adhesion, clay exfoliation and CNT dispersion.

#### 567 *4.4. Electrical Property*

568 Levchenko et al. (2011) adopted both experimental and theoretical approach in  
569 determining the influence of clay (OC) inclusion on electrical percolation threshold of ternary  
570 PP/CNT/OC nanocomposite. Electrical percolation threshold was reported to reduce by  
571 28.4% (from 0.95 to 0.68 vol% of CNT) on incorporation of clay into PP/CNT. The  
572 behaviour was ascribed to clay disentangling and prevention of CNT aggregations during  
573 melt-mix processing, thereby interparticle-contact numbers were enriched to form conductive  
574 network. They corroborated this explanation by morphological study that showed clusters of  
575 clay or CNT in the singly filled PP/OC or PP/CNT composites, respectively (Figs. 9a, b).  
576 Conversely, the SEM image of the ternary showed well-exfoliated CNT at the instance of  
577 clay with an established network structure needed for conductivity (Fig. 9c).

578 On the contrary, Khajehpour et al. (2014) reported an increase of percolation threshold on  
579 addition of clay to CNT/PVDF from 0.3 to 0.5 wt% of CNT due to deterioration of the  
580 conductive network caused by the clay platelets barrier role.



581  
582 **Fig. 9.** SEM image of (a) PP/OC (b) PP/CNT (c) PP/CNT/OC (Levchenko et al., 2011)

#### 583 4.5. Mechanical Properties

584 Zhang et al. (2006) incorporated CNT-clay nanofiller, prepared by CCVD process, into  
585 polyamide-6 (PA6) by melt mixing. Tensile modulus and strength were enhanced  
586 significantly by 289% and 153% respectively. Homogenous dispersion of CNT-Mt was  
587 reported and attributed to swollen and exfoliation of clay by iron ions intercalation into clay  
588 interlayers as well as CNT growth on clay platelets resulted in enhanced mechanical property  
589 of the ternary prepared with 1 wt% of CNT-clay. Olalekan et al. (2010) utilized masterbatch  
590 of polypropylene-clay (PP/clay) and CNT in preparing ternary composite. They reported  
591 PP/clay composite with tensile strength, Young's modulus and impact strength of 28.55 MPa,  
592 1588.27 MPa and 5.55 kJ m<sup>-2</sup>, respectively. With incorporation of CNT alongside Mt, they  
593 achieved improved tensile strength, Young's modulus and impact strength by 27, 42 and 13%  
594 respectively. It was related to higher aspect ratio and specific surface area of the incorporated  
595 CNT, and clay facilitated CNT superior dispersion in the matrix and in turn enhanced the  
596 mechanical properties of the ternary composite. Geng et al. (2012) reinforced PVDF with  
597 CNT and Mt. The mechanical properties of the ternary reportedly surpassed the neat PVDF

598 and single-filled nanocomposites. The reported dynamic mechanical analysis (DMA) showed  
599 that the ternary PVDF/1.9CNT/3Mt had approximately twice mechanical loss factor ( $\tan \delta$ )  
600 than binary composites, with an established conductive network and piezoelectric phase,  
601 which made the ternary to be applicable for damping application.

602 Prashantha et al. (2014) developed polypropylene (P) nanocomposite reinforced with  
603 hybrid (1:1) of Mt (C) and CNT (M). Both binary (MP-2, MP-4, CP-2, CP-4) and ternary  
604 (MCP-2, MCP-4) composites showed increase in strength and modulus with nanofillers  
605 loadings. Meanwhile, composites with the hybrid fillers recorded better improvements in  
606 tensile strength (MCP-2, 37%; MCP-4, 54%) and tensile modulus (MCP-2, 40%; MCP-4,  
607 50%). Also, ternary MCP-2 (CNT 1 wt%; Mt 1 wt%) was reported to have the least  
608 elongation reduction when compared with neat PP due to increased polymer chains rigidity as  
609 a result of nanofillers restriction effects. For hybrid-filled composites, positive synergy in  
610 both flexural strength (MCP-2, 49%; MCP-4, 64%) and modulus (MCP-2, 58%; MCP-4,  
611 65%) were also reported. The notched ternary composites MCP-2 and MCP-4 maintained  
612 respective peak impact strength improvement of 50% and 53% above the neat matrix. The  
613 high mechanical properties of the ternary nanocomposites were related to strong clay-CNT  
614 and fillers-matrix interfacial adhesions revealed by morphology study. Uniform distribution  
615 of retained broken CNT upon failure, instead of pull-out from the matrix, was cited as the  
616 factor for property improvement.

617 Terzopoulou et al. (2016) studied the mechanical behaviour of poly( $\epsilon$ -caprolactone)  
618 incorporated with clay-decorated CNT filler. The hybrid nanofiller was varied: PCL/clay-  
619 CNT 0.5 wt%, PCL/clay-CNT 1.0 wt% and PCL/clay-CNT 2.5 wt%. They reported increase  
620 in yield point and Young's modulus (stiffness) with the increase in fillers loading, which was  
621 related to composite enhanced crystallinity. However, only PCL/clay-CNT 0.5 wt% recorded  
622 increase in elongation with respect to the neat matrix. Also, PCL/clay-CNT 0.5 wt% and

623 PCL/clay-CNT 1.0 wt% had respective 5.5 and 3.7% increase in tensile strength but  
624 PCL/clay-CNT 2.5 wt% showed 15.9% reduction. Apparently, 0.5 wt% clay-CNT enhanced  
625 the composite strength, but higher loading led to weak fillers/PCL interfacial bonding  
626 because of agglomeration.

#### 627 *4.6. Tribology Property*

628 Polymeric nanocomposites are fast replacing the traditional materials in fabricating  
629 mechanical elements (clutches, bush, gear, and bearing) and other electromechanical systems  
630 that solely depend on friction, wear and lubrication principles (Wani et al., 2018). Achieving  
631 high tribology efficiency requires homogenous distribution of fillers within matrix.

632 Azam and Samad (2018b) employed solution mixing in preparing UHMWPE  
633 nanocomposite using hybrid of Mt (C15A) and CNT for marine application. The samples  
634 were designated as Sample, Sample-1, Sample-2, Sample-3, Sample-4, Sample-5, and  
635 Sample-6 representing respectively 1.5wt%C15A/UHMWPE, 0.5wt%CNT/UHMWPE,  
636 1.5wt%CNT/UHMWPE, 3wt%CNT/UHMWPE, 0.5wt%CNT/1.5wt%C15A/UHMWPE,  
637 1.5wt%CNT/1.5wt%C15A/UHMWPE, and 3wt%CNT/1.5wt%C15A/UHMWPE. Cyclic  
638 sliding wear test was performed at 9 N load, underwater. Neat UHMWPE failed as early as  
639 22000 cycles, while none of the binary and ternary composites failed at the condition. By  
640 increasing force to 12 N on composites, they found that only Sample-2 (1.5 wt% CNT) and  
641 Sample-5 (1.5 wt% CNT/1.5 wt% C15A) sustained wear life up to 150000 cycles. The earlier  
642 failure of neat matrix and other samples was either attributed to lack of CNT, inadequate  
643 CNT causing inept matrix chains anchoring, aggregation of CNT or formation of dual-phase  
644 structures. These caused weak filler(s)-matrix bonding and poor bridging of the polymer  
645 chains resulting in an inefficient loading transfer by the CNTs on the course of wear tests.  
646 Interestingly, SEM study of Sample-2 and Sample-5 was reported to reveal homogenous  
647 filler(s) dispersion that promoted matrix-filler interactions, polymer chains bridging, and thus

648 secured against any pull out during wear test. On further investigation of the two samples,  
 649 ternary Sample-5 displayed its superiority up to 300000 cycles, which indicated the  
 650 significant role of the hybrid nanoclay/CNT fillers over single-filled Sample-2 that failed at  
 651 170000 cycles.

652 For Sample-5 (with hybrid nanofillers), clay was said to create a torturous path, due to its  
 653 platelet structure, which prevented water molecule absorption (transportation) while the CNT  
 654 synergistically bridged the polymer chains together during wear test underwater. As hardness  
 655 is a critical factor for high wear property, report of 17.14, 12.4 and 2.7% influence of water  
 656 on the hardness of neat polymer, Sample-2 and Sample-5 respectively confirmed the synergy  
 657 in ternary.

658 **5. Polymer blend reinforced with Mt-CNT Nanofillers**

659 Although this review focusses on a thermoplastic matrix reinforced with Mt-CNT  
 660 nanofillers, it is worth considering that researchers have also incorporated the hybrid fillers  
 661 into polymer blends (Table 2) and reported magnificent properties enhancement.  
 662 Incorporation of Mt/CNT in blend reportedly led to co-continuous morphology formation  
 663 (Potschke et al., 2007; Al-Saleh, 2015), mechanical (Chiu, 2017b) and flammability  
 664 (Ambuken et al., 2014) properties augmentation.

665 **Table 2**

666 Summary of thermoplastics blends filled with hybrid of CNT and Mt.

Matrix		Optimum hybrid filler concentration (wt%)		Dispersion technique	Focused application	References
I	II	CNT	Mt			
PE	PP	1*	1*	Melt-mixing	Electrical & mechanical	Al-Saleh (2015)
PC	PP	2	3	Melt-mixing	Electrical	Pötschke et al. (2007)
PC	PVDF	2	1	Melt-mixing	Thermo-mechanical	Chiu (2017b)
PU	PA-11	3.5	3.5	Melt-mixing	Thermo-mechanical	Ambuken et al. (2014)

667 \*%volume



## 668 **6. Conclusion**

669 This review has provided the advances on high-performance thermoplastics ternary  
670 nanocomposites specifically prepared by the sole incorporation of montmorillonite clays and  
671 carbon nanotubes. Preparation of nanocomposites through the conventional and the recent  
672 approaches was briefly summarized. Systematically, the reviewed studied each of the bulk  
673 properties of nanocomposite: rheology, morphology, thermal, mechanical, electrical, and  
674 tribology. Factors responsible for these properties enhancement were identified, and overall  
675 nanocomposite behaviour was found to be principally hinge on the resulting morphology.

676 The hybrid fillers influence high properties, though how efficient the influence is solely  
677 depended on their level of dispersion within the matrix because agglomeration of any or both  
678 of the nanofillers substantially reduce or cause more detrimental effect on the resulting  
679 nanocomposite. There is no gainsaying in the significant of rheological property of the  
680 composite emanating from right material selection, formulation and other processing  
681 variables.

682 The review established the effectiveness of clay in aiding the dispersion of CNT by  
683 lowering the viscosity of polymer thereby reducing the CNT percolation threshold, which  
684 significantly affects material cost. Clay interjects bundled CNT particles as CNT has a high  
685 degree of affinity for nanoclay. Consequently, aiding the formation of network structures that  
686 favour electrical and thermal conductivity, and restrict polymer chains movement thereby  
687 enhances flame retardancy and mechanical behaviour. Similarly, the presence of CNT  
688 facilitates clay d-value increase that leads to improved exfoliation of clay.

689 However, there is need for more research pertaining to the implications of processing  
690 behaviour on the ternary nanocomposites. Processing factors, such as temperature, shear and  
691 time residence that ultimately affect the resulting nanocomposite properties, should be further  
692 studied while using Mt and CNT as hybrid filler in polymers.

693 The superior reduction of the peak of heat release rate (PHRR) is mostly reported in the  
694 ternary system, which is related to the formation of synergistic uniform crust by Mt-CNT  
695 over the burning composite. Thus limits the heat and gas diffusion and consequently lessen  
696 the nanocomposite flammability. Nanoclay modification processing/chemicals should be  
697 carefully selected as it is majorly cited to be responsible for early degradation of ternary  
698 nanocomposite.

699 For tribology application, clay creates a tortuous path (due to its platelet structure) that  
700 prevents molecule absorption (transportation) by nanocomposite while CNT synergistically  
701 bridged the polymer chains together resulting in improved wear resistance. Another key role  
702 of clay is the creation of polymorph phase in polymer, and CNT inclusion is responsible for  
703 the establishment of co-continuous morphological formation in polymer blend.

704 Thermal conductivity is vital in the design of material for heat management services: it  
705 improves and guarantees the service life of a system as well as the reduction of hazards.  
706 Concurrently, mechanical durability cannot be traded-off in advanced applications such as  
707 aerospace, automobile, military and other thermomechanical facilities.

708 **Declarations of interest:** none

### 709 **Acknowledgements**

710 This work was supported by the Petroleum Technology Development Fund – Nigeria  
711 [Grant Number: 18GFC/PHD/065].

712

713

714

715 **References**

- 716 Abidin, M.S.Z., Herceg, T., Greenhalgh, E.S., Shaffer, M., Bismarck, A., 2019. Enhanced  
717 fracture toughness of hierarchical carbon nanotube reinforced carbon fibre epoxy  
718 composites with engineered matrix microstructure. *Compos. Sci. Technol.* 170, 85–92.  
719 <https://doi.org/10.1016/j.compscitech.2018.11.017>
- 720 Aguzzi, C., Donnadio, A., Quaglia, G., Latterini, L., Viseras, C., Ambrogi, V., 2019.  
721 Halloysite-Doped Zinc Oxide for Enhanced Sunscreening Performance. *ACS Appl.*  
722 *Nano Mater.* xxx, xxx–xxx. <https://doi.org/10.1021/acsanm.9b01482>
- 723 Ahamed, F., Phang, S.W., Sin, T.L., 2016. Mechanical behaviour of thermoplastic  
724 starch/montmorillonite/alumina trihydrate nanocomposites. *J. Eng. Sci. Technol.* 11,  
725 1344–1359.
- 726 Aït Hocine, N., Médéric, P., Aubry, T., 2008. Mechanical properties of polyamide-12 layered  
727 silicate nanocomposites and their relations with structure. *Polym. Test.* 27, 330–339.  
728 <https://doi.org/10.1016/j.polymertesting.2007.12.002>
- 729 Al-Saleh, M.H., 2017. Clay/carbon nanotube hybrid mixture to reduce the electrical  
730 percolation threshold of polymer nanocomposites. *Compos. Sci. Technol.* 149, 34–40.  
731 <https://doi.org/10.1016/j.compscitech.2017.06.009>
- 732 Al-Saleh, M.H., 2015. Effect of Clay Addition on the Properties of Carbon Nanotubes-Filled  
733 Immiscible Polyethylene/Polypropylene Blends. *J. Macromol. Sci. Part B Phys.* 54,  
734 1259–1266. <https://doi.org/10.1080/00222348.2015.1085753>
- 735 Almasri, D.A., Rhadfi, T., Atieh, M.A., McKay, G., Ahzi, S., 2018. High performance  
736 hydroxyiron modified montmorillonite nanoclay adsorbent for arsenite removal. *Chem.*  
737 *Eng. J.* 335, 1–12. <https://doi.org/10.1016/j.cej.2017.10.031>
- 738 Alshammari, B.A., Wilkinson, A., 2016. Impact of carbon nanotubes addition on electrical,  
739 thermal, morphological, and tensile properties of poly (ethylene terephthalate). *Appl.*

740 Petrochemical Res. 6, 257–267. <https://doi.org/10.1007/s13203-016-0161-2>

741 Ambuken, P. V., Stretz, H.A., Koo, J.H., Messman, J.M., Wong, D., 2014. Effect of addition  
742 of montmorillonite and carbon nanotubes on a thermoplastic polyurethane: High  
743 temperature thermomechanical properties. *Polym. Degrad. Stab.* 102, 160–169.  
744 <https://doi.org/10.1016/j.polymdegradstab.2014.01.017>

745 Anbusagar, N.R.R., Palanikumar, K., Ponshanmugakumar, A., 2018. Preparation and  
746 properties of nanopolymer advanced composites: A review, in: Jawaid, M., Khan, M.M.  
747 (Eds.), *Polymer-Based Nanocomposites for Energy and Environmental Applications*.  
748 Woodhead Publishing Series in Composites Science and Engineering, pp. 27–73.  
749 <https://doi.org/10.1016/B978-0-08-102262-7.00002-7>

750 Arrigo, R., Ronchetti, S., Montanaro, L., Malucelli, G., 2018. Effects of the nanofiller size  
751 and aspect ratio on the thermal and rheological behaviour of PEG nanocomposites  
752 containing boehmites or hydrotalcites. *J. Therm. Anal. Calorim.* 134, 1667–1680.  
753 <https://doi.org/10.1007/s10973-018-7555-6>

754 Avilés, F., Cauich-Rodríguez, J. V., Toro-Estay, P., Yazdani-Pedram, M., Aguilar-Bolados,  
755 H., 2018. Improving carbon nanotube/polymer interactions in nanocomposites, in:  
756 Rafiee, R. (Ed.), *Carbon Nanotube-Reinforced Polymers From Nanoscale to*  
757 *Macroscale*. Elsevier, pp. 83–115. <https://doi.org/10.1016/B978-0-323-48221-9.00005-4>

758 Aydoğan, B., Usta, N., 2019. Fire behaviour assessment of rigid polyurethane foams  
759 containing nanoclay and intumescent flame retardant based on cone calorimeter tests. *J.*  
760 *Chem. Technol. Metall.* 54, 55–63.  
761 [https://doi.org/https://dl.uctm.edu/journal/node/j2019-1/7\\_17\\_223\\_p\\_55\\_63.pdf](https://doi.org/https://dl.uctm.edu/journal/node/j2019-1/7_17_223_p_55_63.pdf)

762 Azam, M.U., Samad, M.A., 2018a. A novel organoclay reinforced UHMWPE nanocomposite  
763 coating for tribological applications. *Prog. Org. Coatings* 118, 97–107.  
764 <https://doi.org/10.1016/j.porgcoat.2018.01.028>

765 Azam, M.U., Samad, M.A., 2018b. UHMWPE hybrid nanocomposite coating reinforced with  
766 nanoclay and carbon nanotubes for tribological applications under water with/without  
767 abrasives. *Tribol. Int.* 124, 145–155. <https://doi.org/10.1016/j.triboint.2018.04.003>

768 Barick, A.K., Tripathy, D.K., 2011. Effect of organically modified layered silicate nanoclay  
769 on the dynamic viscoelastic properties of thermoplastic polyurethane nanocomposites.  
770 *Appl. Clay Sci.* 52, 312–321. <https://doi.org/10.1016/j.clay.2011.03.010>

771 Beyer, G., 2006. Flame retardancy of nanocomposites based on organoclays and carbon  
772 nanotubes with aluminum trihydrate. *Polym. Adv. Technol.* 17, 218–225.  
773 <https://doi.org/10.1002/pat.696>

774 Beyer, G., 2005. Filler blend of carbon nanotubes and organoclays with improved char as a  
775 new flame retardant system for polymers and cable applications. *Fire Mater.* 29, 61–69.  
776 <https://doi.org/10.1002/fam.866>

777 Bischoff, E., Goncalves, G.P.O., Simon, D.A., Schrekker, H.S., Lavorgna, M., Ambrosio, L.,  
778 Liberman, S.A., Mauler, R.S., 2017. Unrevealing the effect of different dispersion  
779 agents on the properties of ethylene-propylene copolymer/halloysite nanocomposites.  
780 *Mater. Des.* 131, 232–241.  
781 <https://doi.org/https://dx.doi.org/10.1016/j.matdes.2017.06.033>

782 Boumbimba, R.M., Coulibaly, M., Peng, Y., N'souglo, E.K., Wang, K., Gerard, P., 2018.  
783 Investigation of the impact response of PMMA-based nano-rubbers under various  
784 temperatures. *J. Polym. Res.* 25, 76. <https://doi.org/10.1007/s10965-018-1479-5>

785 Bourbigot, S., Sarazin, J., Samyn, F., Jimenez, M., 2019. Intumescent ethylene-vinyl acetate  
786 copolymer: Reaction to fire and mechanistic aspects. *Polym. Degrad. Stab.* 161, 235–  
787 244. <https://doi.org/10.1016/j.polymdegradstab.2019.01.029>

788 Bray, D.J., Dittanet, P., Guild, F.J., Kinloch, A.J., Masania, K., Pearson, R.A., Taylor, A.C.,  
789 2013. The modelling of the toughening of epoxy polymers via silica nanoparticles: The

790 effects of volume fraction and particle size. *Polymer (Guildf)*. 54, 7022–7032.  
791 <https://doi.org/10.1016/j.polymer.2013.10.034>

792 Brown, T.D., Dalton, P.D., Hutmacher, D.W., 2016. Melt electrospinning today: An  
793 opportune time for an emerging polymer process. *Prog. Polym. Sci.* 56, 116–166.  
794 <https://doi.org/10.1016/j.progpolymsci.2016.01.001>

795 Bunekar, N., Tsai, T., Huang, J., Chen, S., 2018. Investigation of thermal, mechanical and gas  
796 barrier properties of polypropylene-modified clay nanocomposites by micro-  
797 compounding process. *J. Taiwan Inst. Chem. Eng.* 88, 252–260.  
798 <https://doi.org/https://doi.org/10.1016/j.jtice.2018.04.016>

799 Cao, M., Du, C., Guo, H., Songa, S., Li, X., Li, B., 2019. Continuous network of CNTs in  
800 poly(vinylidene fluoride) composites with high thermal and mechanical performance for  
801 heat exchangers. *Compos. Sci. Technol.* 173, 33–40.  
802 <https://doi.org/10.1016/j.compscitech.2019.01.023>

803 Chatterjee, S., Nafezarefi, F., Tai, N.H., Schlagenhaut, L., Nüesch, F.A., Chu, B.T.T., 2012.  
804 Size and synergy effects of nanofiller hybrids including graphene nanoplatelets and  
805 carbon nanotubes in mechanical properties of epoxy composites. *Carbon N. Y.* 50,  
806 5380–5386. <https://doi.org/10.1016/j.carbon.2012.07.021>

807 Chen, H., Ginzburg, V. V, Yang, J., Yang, Y., Liu, W., Huang, Y., Du, L., Chen, B., 2016.  
808 Thermal conductivity of polymer-based composites: Fundamentals and applications.  
809 *Prog. Polym. Sci.* 59, 41–85. <https://doi.org/10.1016/j.progpolymsci.2016.03.001>

810 Chiu, F., 2017a. Halloysite nanotube- and organoclay-filled biodegradable poly(butylene  
811 succinate-co-adipate)/maleated polyethylene blend- based nanocomposites with  
812 enhanced rigidity. *Compos. Part B* 110, 193–203.

813 Chiu, F., 2017b. Poly(vinylidene fluoride)/polycarbonate blend-based nanocomposites with  
814 enhanced rigidity - Selective localization of carbon nanofillers and organoclay. *Polym.*

815 Test. 62, 115–123.  
816 <https://doi.org/http://dx.doi.org/10.1016/j.polymeresting.2017.06.018>

817 Chiu, F.C., 2016. Fabrication and characterization of biodegradable poly(butylene succinate-  
818 co-adipate) nanocomposites with halloysite nanotube and organo-montmorillonite as  
819 nanofillers. *Polym. Test.* 54, 1–11. <https://doi.org/10.1016/j.polymeresting.2016.06.018>

820 Chiu, F.C., 2014. Comparisons of phase morphology and physical properties of PVDF  
821 nanocomposites filled with organoclay and/or multi-walled carbon nanotubes. *Mater.*  
822 *Chem. Phys.* 143, 681–692. <https://doi.org/10.1016/j.matchemphys.2013.09.054>

823 Cicco, D.D., Asaee, Z., Taheri, F., 2017. Use of nanoparticles for enhancing the interlaminar  
824 properties of fibre-reinforced composites and adhesively bonded joints-a review.  
825 *Nanomaterials* 7, 360. <https://doi.org/10.3390/nano7110360>

826 Das, S., Samal, S.K., Mohanty, S., Nayak, S.K., 2018. Crystallization of polymer blend  
827 nanocomposites, in: Thomas, K.S., Mohammed, A.P., Gowd, E.B., Kalarikkal, N.  
828 (Eds.), *Crystallization in Multiphase Polymer Systems*. Elsevier Inc., pp. 313–339.  
829 <https://doi.org/10.1016/B978-0-12-809453-2.00011-6>

830 Dasari, A., Yu, Z.Z., Cai, G.P., Mai, Y.W., 2013. Recent developments in the fire retardancy  
831 of polymeric materials. *Prog. Polym. Sci.* 38, 1357–1387.  
832 <https://doi.org/10.1016/j.progpolymsci.2013.06.006>

833 Dlamini, D.S., Li, J., Mamba, B.B., 2019. Critical review of montmorillonite/polymer mixed-  
834 matrix filtration membranes: Possibilities and challenges. *Appl. Clay Sci.* 168, 21–30.  
835 <https://doi.org/10.1016/j.clay.2018.10.016>

836 Edenharter, A., Feicht, P., Diar-Bakerly, B., Beyer, G., Breu, J., 2016. Superior flame  
837 retardant by combining high aspect ratio layered double hydroxide and graphene oxide.  
838 *Polymer (Guildf)*. 91, 41–49. <https://doi.org/10.1016/j.polymer.2016.03.020>

839 El Rhazi, M., Majid, S., Elbasri, M., Salih, F.E., Oularbi, L., Lafdi, K., 2018. Recent progress

840 in nanocomposites based on conducting polymer: application as electrochemical sensors.  
841 Int. Nano Lett. 8, 79–99. <https://doi.org/10.1007/s40089-018-0238-2>

842 Enotiadis, A., Litina, K., Gournis, D., Rangou, S., Avgeropoulos, A., Xidas, P.,  
843 Triantafyllidis, K., 2013. Nanocomposites of polystyrene-b-poly(isoprene)-b-  
844 polystyrene triblock copolymer with clay-carbon nanotube hybrid nanoadditives. J.  
845 Phys. Chem. B 117, 907–915. <https://doi.org/10.1021/jp309361b>

846 Fang, C., Zhang, J., Chen, X., Weng, G.J., 2019. A Monte Carlo model with equipotential  
847 approximation and tunneling resistance for the electrical conductivity of carbon  
848 nanotube polymer composites. Carbon N. Y. 146, 125–138.  
849 <https://doi.org/10.1016/j.carbon.2019.01.098>

850 Fanga, F., Ran, S., Fang, Z., Song, P., Wang, H., 2019. Improved flame resistance and  
851 thermo-mechanical properties of epoxy resin nanocomposites from functionalized  
852 graphene oxide via self-assembly in water. Compos. Part B 165, 406–416.  
853 <https://doi.org/https://doi.org/10.1016/j.compositesb.2019.01.086>

854 Feng, Y., He, C., Wen, Y., Ye, Y., Zhou, X., Xie, X., Mai, Y.-W., 2018. Superior flame  
855 retardancy and smoke suppression of epoxy-based composites with phosphorus/nitrogen  
856 co-doped graphene. J. Hazard. Mater. 346, 140–151.  
857 <https://doi.org/10.1016/j.jhazmat.2017.12.019>

858 Geng, C., Wang, J., Zhang, Q., Fu, Q., 2012. New piezoelectric damping composites of  
859 poly(vinylidene fluoride) blended with clay and multi-walled carbon nanotubes. Polym.  
860 Int. 61, 934–938. <https://doi.org/10.1002/pi.4161>

861 Golgoon, A., Aliofkhazraei, M., Toorani, M., Moradi, M.H., Rouhaghdam, A.S., 2015.  
862 Corrosion and Wear Properties of Nanoclay- polyester Nanocomposite Coatings  
863 Fabricated by Electrostatic Method. Procedia Mater. Sci. 11, 536–541.  
864 <https://doi.org/10.1016/j.mspro.2015.11.042>



865 Gorrasi, G., D'Ambrosio, S., Patimo, G., Pantani, R., 2014. Hybrid clay-carbon  
866 nanotube/PET composites: Preparation, processing, and analysis of physical properties.  
867 J. Appl. Polym. Sci. 131, 1–7. <https://doi.org/10.1002/app.40441>

868 Gorrasi, G., Milone, C., Piperopoulos, E., Lanza, M., Sorrentino, A., 2013. Hybrid clay  
869 mineral-carbon nanotube-PLA nanocomposite films. Preparation and photodegradation  
870 effect on their mechanical, thermal and electrical properties. Appl. Clay Sci. 71, 49–54.  
871 <https://doi.org/10.1016/j.clay.2012.11.004>

872 Gorrasi, G., Sorrentino, A., 2015. Mechanical milling as a technology to produce structural  
873 and functional bio-nanocomposites. Green Chem. 17, 2610-2625.  
874 <https://doi.org/10.1039/c5gc00029g>

875 Han, X., Zeng, X., Wang, J., Kong, D., Foster, N.R., Chen, J., 2016. Transparent flexible  
876 ZnO/MWCNTs/pbma ternary nanocomposite film with enhanced mechanical properties.  
877 Sci. China Chem. 59, 1010–1017. <https://doi.org/10.1007/s11426-015-0467-4>

878 Hapuarachchi, T.D., Peijs, T., 2010. Multiwalled carbon nanotubes and sepiolite nanoclays as  
879 flame retardants for polylactide and its natural fibre reinforced composites. Compos.  
880 Part A Appl. Sci. Manuf. 41, 954–963.  
881 <https://doi.org/10.1016/j.compositesa.2010.03.004>

882 Hosseini, S.M., Yousefi, A.A., 2017a. Piezoelectric sensor based on electrospun PVDF-  
883 MWCNT-Cloisite 30B hybrid nanocomposites. Org. Electron. 50, 121–129.  
884 <https://doi.org/10.1016/j.orgel.2017.07.035>

885 Hosseini, S.M., Yousefi, A.A., 2017b. Electrospun PVDF/MWCNT/OMMT hybrid  
886 nanocomposites: preparation and characterization. Iran. Polym. J. 26, 331–339.  
887 <https://doi.org/10.1007/s13726-017-0522-4>

888 Isitman, N.A., Kaynak, C., 2010. Nanoclay and carbon nanotubes as potential synergists of  
889 an organophosphorus flame-retardant in poly(methyl methacrylate). Polym. Degrad.

890 Stab. 95, 1523–1532. <https://doi.org/10.1016/j.polymdegradstab.2010.06.013>

891 Jaafar, M., 2017. Development of Hybrid Fillers/Polymer Nanocomposites for Electronic  
892 Applications, in: Srivastava, S.K., Mittal, V. (Eds.), Hybrid Nanomaterials: Advances in  
893 Energy, Environment and Polymer Nanocomposites. Scrivener , Wiley, pp. 349–369.  
894 <https://doi.org/10.1002/9781119160380.ch7>

895 Ji, X., Chen, D., Wang, Q., Shen, J., Guo, S., 2018. Synergistic effect of flame retardants and  
896 carbon nanotubes on flame retarding and electromagnetic shielding properties of  
897 thermoplastic polyurethane. *Compos. Sci. Technol.* 163, 49–55.  
898 <https://doi.org/https://doi.org/10.1016/j.compscitech.2018.05.007>

899 Kausar, A., 2016. Novel Polyamide Nanocomposite with Montmorillonite Clay and Gold  
900 Nanoparticle Nanofillers. *Nanosci. Nanotechnol.* 6, 43–47.  
901 <https://doi.org/10.5923/j.nn.20160603.02>

902 Kausar, A., Rafique, I., Muhammad, B., 2017. Aerospace Application of Polymer  
903 Nanocomposite with Carbon nanotube, Graphite, Graphene Oxide and Nanoclay.  
904 *Polym. Plast. Technol. Eng.* 56, 1438–1456.  
905 <https://doi.org/https://doi.org/10.1080/03602559.2016.1276594>

906 Khajehpour, M., Arjmand, M., Sundararaj, U., 2014. Dielectric properties of multiwalled  
907 carbon nanotube/ clay/polyvinylidene fluoride nanocomposites: effect of clay  
908 incorporation. *Polym. Compos.* 37, 161–167. <https://doi.org/10.1002/pc.23167>

909 Khan, S., Bedi, H.S., Agnihotri, P.K., 2018. Augmenting mode-II fracture toughness of  
910 carbon fibre/epoxy composites through carbon nanotube grafting. *Eng. Fract. Mech.*  
911 204, 211–220. <https://doi.org/10.1016/j.engfracmech.2018.10.014>

912 Kim, H.S., Jang, J.U., Yu, J., Kim, S.Y., 2015. Thermal conductivity of polymer composites  
913 based on the length of multi-walled carbon nanotubes. *Compos. Part B Eng.* 79, 505–  
914 512. <https://doi.org/10.1016/j.compositesb.2015.05.012>

915 Klonos, P., Pissis, P., 2017. Effects of interfacial interactions and of crystallization on rigid  
916 amorphous fraction and molecular dynamics in polylactide/silica nanocomposites: A  
917 methodological approach. *Polymer (Guildf)*. 112, 228–243.  
918 <https://doi.org/10.1016/j.polymer.2017.02.003>

919 Kumar, A., Kumar, K., Ghosh, P.K., Yadav, K.L., 2018. MWCNT/TiO<sub>2</sub> hybrid nano filler  
920 toward high-performance epoxy composite. *Ultrason. Sonochem.* 41, 37–46.  
921 <https://doi.org/10.1016/j.ultsonch.2017.09.005>

922 Kumar, S., Sun, L.L., Caceres, S., Li, B., Wood, W., Perugini, A., Maguire, R.G., Zhong,  
923 W.H., 2010. Dynamic synergy of graphitic nanoplatelets and multi-walled carbon  
924 nanotubes in polyetherimide nanocomposites. *Nanotechnology* 21, 105702.  
925 <https://doi.org/10.1088/0957-4484/21/10/105702>

926 Kurahatti, R. V., Surendranathan, A.O., Kori, S.A., Singh, N., Kumar, A.V.R., Srivastava, S.,  
927 2010. Defence applications of polymer nanocomposites. *Def. Sci. J.* 60, 551–563.  
928 <https://doi.org/10.14429/dsj.60.578>

929 Lee, S., Kim, H. min, Seong, D.G., Lee, D., 2019. Synergistic improvement of flame  
930 retardant properties of expandable graphite and multi-walled carbon nanotube reinforced  
931 intumescent polyketone nanocomposites. *Carbon N. Y.* 143, 650–659.  
932 <https://doi.org/10.1016/j.carbon.2018.11.050>

933 Levchenko, V., Mamunya, Y., Boiteux, G., Lebovka, M., Alcouffe, P., Seytre, G., Lebedev,  
934 E., 2011. Influence of organo-clay on electrical and mechanical properties of  
935 PP/MWCNT/OC nanocomposites. *Eur. Polym. J.* 47, 1351–1360.  
936 <https://doi.org/10.1016/j.eurpolymj.2011.03.012>

937 Li, Y., Zhang, H., Liu, Y., Wang, H., Huang, Z., Peijs, T., Bilotti, E., 2018. Synergistic  
938 effects of spray-coated hybrid carbon nanoparticles for enhanced electrical and thermal  
939 surface conductivity of CFRP laminates. *Compos. Part A* 105, 9–18.

940 <https://doi.org/https://doi.org/10.1016/j.compositesa.2017.10.032>

941 Liu, L., Grunlan, J.C., 2007. Clay assisted dispersion of carbon nanotubes in conductive  
942 epoxy nanocomposites. *Adv. Funct. Mater.* 17, 2343–2348.  
943 <https://doi.org/10.1002/adfm.200600785>

944 Liu, W., Chen, Z., Cheng, X., Wang, Y., Amankwa, A.R., Xu, J., 2016. Design and ballistic  
945 penetration of the ceramic composite armor. *Compos. Part B Eng.* 84, 33–40.  
946 <https://doi.org/10.1016/j.compositesb.2015.08.071>

947 Liu, X., Guo, J., Tang, W., Li, H., Gu, X., Sun, J., Zhang, S., 2019. Enhancing the flame  
948 retardancy of thermoplastic polyurethane by introducing montmorillonite nanosheets  
949 modified with phosphorylated chitosan. *Compos. Part A* 119, 291–298.  
950 <https://doi.org/https://doi.org/10.1016/j.compositesa.2019.02.009>

951 López-Barroso, J., Martínez-Hernández, A.L., Rivera-Armenta, J.L., Velasco-Santos, C.,  
952 2018. Multidimensional nanocomposites of epoxy reinforced with 1D and 2D carbon  
953 nanostructures for improve fracture resistance. *Polymers* 10, 281.  
954 <https://doi.org/10.3390/polym10030281>

955 Ma, H., Tong, L., Xu, Z., Fang, Z., 2007. Synergistic effect of carbon nanotube and clay for  
956 improving the flame retardancy of ABS resin. *Nanotechnology* 18, 375602.  
957 <https://doi.org/10.1088/0957-4484/18/37/375602>

958 Madaleno, L., Pyrz, R., Crosky, A., Jensen, L.R., Rauhe, J.C.M., Dolomanova, V., Timmons,  
959 A.M.M.V. de B., Pinto, J.J.C., Norman, J., 2013. Processing and characterization of  
960 polyurethane nanocomposite foam reinforced with montmorillonite-carbon nanotube  
961 hybrids. *Compos. Part A Appl. Sci. Manuf.* 44, 1–7.  
962 <https://doi.org/10.1016/j.compositesa.2012.08.015>

963 Madaleno, L., Pyrz, R., Jensen, L.R., Pinto, J.J.C., Lopes, A.B., Dolomanova, V., Schjødt-  
964 Thomsen, J., Rauhe, J.C.M., 2012. Synthesis of clay-carbon nanotube hybrids: Growth

965 of carbon nanotubes in different types of iron modified montmorillonite. *Compos. Sci.*  
966 *Technol.* 72, 377–381. <https://doi.org/10.1016/j.compscitech.2011.11.027>

967 Manikandan, D., Mangalaraja, R.V., Avila, R.E., Siddheswaran, R., Ananthakumar, S., 2012.  
968 Carbon nanotubes rooted montmorillonite (CNT-MM) reinforced nanocomposite  
969 membrane for PEM fuel cells. *Mater. Sci. Eng. B Solid-State Mater. Adv. Technol.* 177,  
970 614–618. <https://doi.org/10.1016/j.mseb.2012.02.027>

971 Manikandan, D., Viswanathan, R., Avila, R.E., Siddheswaran, R., Ananthakumar, S., 2013.  
972 Montmorillonite – carbon nanotube nanofillers by acetylene decomposition using  
973 catalytic CVD. *Appl. Clay Sci.* 71, 37–41. <https://doi.org/10.1016/j.clay.2012.10.001>

974 Marquis, D.M., Guillaume, E., Chivas-Joly, C., 2011. Properties of nanofillers in polymer,  
975 Nanocomposites and polymers with analytical methods, in: Cuppoletti, J. (Ed.), .  
976 *InTech*, Croatia. <https://doi.org/10.5772/21694>

977 Mayeen, A., Shaji, L.K., Nair, A.K., Kalarikkal, N., 2018. Morphological Characterization of  
978 Nanomaterials, in: Bhagyaraj, S.M., Oluwafemi, O.S., Kalarikkal, N., Thomas, S. (Eds.),  
979 *Characterization of Nanomaterials*. Elsevier Ltd., pp. 335–364.  
980 <https://doi.org/10.1016/B978-0-08-101973-3.00012-2>

981 McCrum, N.G., Buckley, C.P., Bucknall, C.B., 1988. Principles of polymer engineering,  
982 *Journal of Non-Newtonian Fluid Mechanics*. Oxford University Press, New York.  
983 [https://doi.org/10.1016/0377-0257\(91\)80013-A](https://doi.org/10.1016/0377-0257(91)80013-A)

984 Moghri, M., Shamaee, H., Shahrajabian, H., Ghannadzadeh, A., 2015. The effect of different  
985 parameters on mechanical properties of PA-6/clay nanocomposite through genetic  
986 algorithm and response surface methods. *Int. Nano Lett.* 5, 133–140.  
987 <https://doi.org/10.1007/s40089-015-0146-7>

988 Mohammed, N.A., 2014. Rheology, Processing and Properties of Polymer Nanocomposites  
989 Based on POSS and Boehmite. PhD Thesis: Technische Universität, Berlin.

990 <https://doi.org/http://dx.doi.org/10.14279/depositonce-3981>

991 Navidfar, A., Sancak, A., Yildirim, K.B., Trabzon, L., 2017. A Study on Polyurethane Hybrid  
992 Nanocomposite Foams Reinforced with Multiwalled Carbon Nanotubes and Silica  
993 Nanoparticles. *Polym. - Plast. Technol. Eng.* 57, 1463–1473.  
994 <https://doi.org/10.1080/03602559.2017.1410834>

995 Nayak, S., 2019. Dielectric Properties of Polymer -Carbon Composites, in: Rahaman, M.,  
996 Khastgir, D., Aldalbahi, A.K. (Eds.), *Carbon-Containing Polymer Composites*. Springer  
997 Series on Polymer and Composite Materials, Springer, Singapore, pp. 211–234.  
998 [https://doi.org/https://doi.org/10.1007/978-981-13-2688-2\\_6](https://doi.org/https://doi.org/10.1007/978-981-13-2688-2_6)

999 Nurul, M.S., Mariatti, M., 2013. Effect of hybrid nanofillers on the thermal, mechanical, and  
1000 physical properties of polypropylene composites. *Polym. Bull.* 70, 871–884.  
1001 <https://doi.org/10.1007/s00289-012-0893-9>

1002 Olalekan, S.T., Muyibi, S.A., Shah, Q.H., Alkhatib, F.M., Yusof, F., Qudsieh, I.Y., 2010.  
1003 Improving the Polypropylene-Clay Composite Using Carbon Nanotubes as Secondary  
1004 Filler. *Energy Res. J.* 1, 68–72.

1005 Oliveira, A.D., Beatrice, C.A.G., Passador, F.R., Pessan, L.A., 2016. Polyetherimide-based  
1006 nanocomposites materials for hydrogen storage. *AIP Conf. Proc.* 1779, 040006.  
1007 <https://doi.org/10.1063/1.4965497>

1008 Pan, H., Pan, Y., Wang, W., Song, L., Hu, Y., Liew, K.M., 2014. Synergistic effect of layer-  
1009 by-layer assembled thin films based on clay and carbon nanotubes to reduce the  
1010 flammability of flexible polyurethane foam. *Ind. Eng. Chem. Res.* 53, 14315–14321.  
1011 <https://doi.org/10.1021/ie502215p>

1012 Pandey, P., Mohanty, S., Nayak, S.K., 2014. Improved flame retardancy and thermal stability  
1013 of polymer/clay nanocomposites, with the incorporation of multiwalled carbon nanotube  
1014 as secondary filler: Evaluation of hybrid effect of nanofillers. *High Perform. Polym.* 26,

1015 826–836. <https://doi.org/10.1177/0954008314531802>

1016 Papageorgiou, D.G., Kinloch, I.A., Young, R.J., 2017a. Mechanical properties of graphene  
1017 and graphene-based nanocomposites. *Prog. Mater. Sci.* 90, 75–127.  
1018 <https://doi.org/10.1016/j.pmatsci.2017.07.004>

1019 Papageorgiou, D.G., Kinloch, I.A., Young, R.J., 2017b. Mechanical properties of graphene  
1020 and graphene-based nanocomposites. *Prog. Mater. Sci.* 90, 75–127.  
1021 <https://doi.org/http://dx.doi.org/10.1016/j.pmatsci.2017.07.004>

1022 Paszkiewicz, S., Szymczyk, A., Sui, X.M., Wagner, H.D., Linares, A., Cirera, A., Varea, A.,  
1023 Ezquerro, T.A., Rosłaniec, Z., 2017. Electrical conductivity and transparency of polymer  
1024 hybrid nanocomposites based on poly(trimethylene terephthalate) containing single  
1025 walled carbon nanotubes and expanded graphite. *J. Appl. Polym. Sci.* 134, 44370.  
1026 <https://doi.org/10.1002/app.44370>

1027 Peeterbroeck, S., Alexandre, M., Nagy, J.B., Pirlot, C., Fonseca, A., Moreau, N., Philippin,  
1028 G., Delhalle, J., Mekhalif, Z., Sporken, R., Beyer, G., Dubois, P., 2004. Polymer-layered  
1029 silicate-carbon nanotube nanocomposites: Unique nanofiller synergistic effect. *Compos.*  
1030 *Sci. Technol.* 64, 2317–2323. <https://doi.org/10.1016/j.compscitech.2004.01.020>

1031 Pitchan, M.K., Bhowmik, S., Balachandran, M., Abraham, M., 2017. Process optimization of  
1032 functionalized MWCNT/polyetherimide nanocomposites for aerospace application.  
1033 *Mater. Des.* 127, 193–203. <https://doi.org/10.1016/j.matdes.2017.04.081>

1034 Pötschke, P., Kretschmar, B., Janke, A., 2007. Use of carbon nanotube filled polycarbonate  
1035 in blends with montmorillonite filled polypropylene. *Compos. Sci. Technol.* 67, 855–  
1036 860. <https://doi.org/10.1016/j.compscitech.2006.02.034>

1037 Potts, J.R., Lee, S.H., Alam, T.M., An, J., Stoller, M.D., Piner, R.D., Ruoff, R.S., 2011.  
1038 Thermomechanical properties of chemically modified graphene/poly(methyl  
1039 methacrylate) composites made by in situ polymerization. *Carbon N. Y.* 49, 2615–2623.

- 1040 <https://doi.org/10.1016/j.carbon.2011.02.023>
- 1041 Prasad, K.E., Das, B., Maitra, U., Ramamurty, U., Rao, C.N.R., 2009. Extraordinary synergy  
1042 in the mechanical properties of polymer matrix composites reinforced with 2  
1043 nanocarbons. *Proc. Natl. Acad. Sci.* 106, 13186–13189.  
1044 <https://doi.org/10.1073/pnas.0905844106>
- 1045 Prashantha, K., Soulestin, J., Lacrampe, M.F., Krawczak, P., 2014. Processing and  
1046 Characterization of Polypropylene Filled with Multiwalled Carbon Nanotube and Clay  
1047 Hybrid Nanocomposites. *Int. J. Polym. Anal. Charact.* 19, 363–371.  
1048 <https://doi.org/10.1080/1023666X.2014.902715>
- 1049 Punetha, V.D., Rana, S., Yoo, H.J., Chaurasia, A., McLeskey, J.T., Ramasamy, M.S., Sahoo,  
1050 N.G., Cho, J.W., 2017. Functionalization of carbon nanomaterials for advanced polymer  
1051 nanocomposites: A comparison study between CNT and graphene. *Prog. Polym. Sci.* 67,  
1052 1–47. <https://doi.org/10.1016/j.progpolymsci.2016.12.010>
- 1053 Radmanesh, F., Rijnaarts, T., Moheb, A., Sadeghi, M., de Vos, W.M., 2019. Enhanced  
1054 selectivity and performance of heterogeneous cation exchange membranes through  
1055 addition of sulfonated and protonated Montmorillonite. *J. Colloid Interface Sci.* 533,  
1056 658–670. <https://doi.org/10.1016/j.jcis.2018.08.100>
- 1057 Raee, E., Kaffashi, B., 2018. Biodegradable polypropylene/thermoplastic starch  
1058 nanocomposites incorporating halloysite nanotubes. *J. Appl. Polym. Sci.* 135, 45740.  
1059 <https://doi.org/10.1002/app.45740>
- 1060 Rahmaoui, F.E.Z., Mederic, P., Aït Hocine, N., Aït Saada, A., Poirot, N., Belaidi, I., 2017.  
1061 Applied Clay Science Contribution of the organo-montmorillonite / graphene pair to the  
1062 rheological and mechanical properties of polyethylene matrix based nanocomposites.  
1063 *Appl. Clay Sci.* 150, 244–251. <https://doi.org/10.1016/j.clay.2017.09.037>
- 1064 Raji, M., Mekhzoum, M.E.M., Qaiss, A.K., Bouhfid, R., 2016. Nanoclay Modification and



1065 Functionalization for Nanocomposites Development: Effect on the Structural,  
1066 Morphological, Mechanical and Rheological Properties, in: Jawaid, M., Qaiss, A.,  
1067 Bouhfid, R. (Eds.), Nanoclay Reinforced Polymer Composites, Engineering Materials.  
1068 Springer, Singapore, pp. 1–34. <https://doi.org/10.1007/978-981-10-1953-1>

1069 Raji, M., Mekhzouma, M.M., Rodrigue, D., Qaissa, A., Bouhfi, R., 2018. Effect of silane  
1070 functionalization on properties of polypropylene/clay nanocomposites. *Compos. Part B*  
1071 146, 106–115. <https://doi.org/10.1016/j.compositesb.2018.04.013>

1072 Ramazanov, M.A., Maharramov, A.M., Ali-zada, R.A., Shirinova, H.A., Hajiyeva, F. V.,  
1073 2018. Theoretical and experimental investigation of the magnetic properties of  
1074 polyvinylidene fluoride and magnetite nanoparticles-based nanocomposites. *J. Theor.*  
1075 *Appl. Phys.* 12, 7–13. <https://doi.org/10.1007/s40094-018-0282-3>

1076 Rao, B.N., Praveen, T.A., Sailaja, R.R.N., Khan, M.A., 2015. HDPE Nanocomposites Using  
1077 Nanoclay, MWCNT and Intumescent Flame Retardant Characteristics, in: 2015 IEEE  
1078 11th International Conference on the Properties and Applications of Dielectric Materials  
1079 (ICPADM). pp. 812–815. <https://doi.org/10.1109/icpadm.2015.7295396>

1080 Ray, S.S., Okamoto, M., 2003. Polymer/layered silicate nanocomposites: A review from  
1081 preparation to processing. *Prog. Polym. Sci.* 28, 1539–1641.  
1082 <https://doi.org/10.1016/j.progpolymsci.2003.08.002>

1083 Ren, J., Dang, K.M., Pollet, E., Avérous, L., 2018. Preparation and characterization of  
1084 thermoplastic potato starch/halloysite nano-biocomposites: Effect of plasticizer nature  
1085 and nanoclay content. *Polymers (Basel)*. 10. <https://doi.org/10.3390/polym10080808>

1086 Roes, A.L., Marsili, E., Nieuwlaar, E., Patel, M.K., 2007. Environmental and cost assessment  
1087 of a polypropylene nanocomposite. *J. Polym. Environ.* 15, 212–226.  
1088 <https://doi.org/10.1007/s10924-007-0064-5>

1089 Rotheron, R.N., Hornsby, P.R., 1996. Flame retardant effects of magnesium hydroxide. *Polym.*

1090 Degrad. Stab. 54, 383–385. [https://doi.org/10.1016/S0141-3910\(96\)00067-5](https://doi.org/10.1016/S0141-3910(96)00067-5)

1091 Rueda, M.M., Auscher, M.C., Fulchiron, R., Périé, T., Martin, G., Sonntag, P., Cassagnau, P.,  
1092 2017. Rheology and applications of highly filled polymers: A review of current  
1093 understanding. Prog. Polym. Sci. 66, 22–53.  
1094 <https://doi.org/10.1016/j.progpolymsci.2016.12.007>

1095 Sa, K., Mahakul, P.C., Subramanyam, B.V.R.S., Raiguru, J., Das, S., Alam, I., Mahanandia,  
1096 P., 2018. Effect of reduced graphene oxide-carbon nanotubes hybrid nanofillers in  
1097 mechanical properties of polymer nanocomposites. IOP Conf. Ser. Mater. Sci. Eng. 338,  
1098 012055. <https://doi.org/10.1088/1757-899X/338/1/012055>

1099 Safdari, M., Al-haik, M.S., 2018. A Review on Polymeric Nanocomposites: Effect of  
1100 Hybridization and Synergy on Electrical Properties, in: Ismail, A.F., Goh, P.S. (Eds.),  
1101 Carbon-Based Polymer Nanocomposites for Environmental and Energy Applications.  
1102 Elsevier, Amsterdam, pp. 113–146. [https://doi.org/10.1016/B978-0-12-813574-7.00005-](https://doi.org/10.1016/B978-0-12-813574-7.00005-8)  
1103 8

1104 Safdari, M., Al-Haik, M.S., 2013. Synergistic electrical and thermal transport properties of  
1105 hybrid polymeric nanocomposites based on carbon nanotubes and graphite  
1106 nanoplatelets. Carbon N. Y. 64, 111–121. <https://doi.org/10.1016/j.carbon.2013.07.042>

1107 Santangelo, S., Gorrasi, G., Di Lieto, R., De Pasquale, S., Patimo, G., Piperopoulos, E.,  
1108 Lanza, M., Faggio, G., Mauriello, F., Messina, G., Milone, C., 2011. Polylactide and  
1109 carbon nanotubes/smectite-clay nanocomposites: Preparation, characterization, sorptive  
1110 and electrical properties. Appl. Clay Sci. 53, 188–194.  
1111 <https://doi.org/10.1016/j.clay.2010.12.013>

1112 Seghar, S., Azem, S., Aït Hocine, N., 2011. Effects of clay nanoparticles on the mechanical  
1113 and physical properties of unsaturated polyester. Adv. Sci. Lett. 4, 3424–3430.  
1114 <https://doi.org/10.1166/asl.2011.2051>

- 1115 Shabanian, M., Hajibeygi, M., Hedayati, K., Khaleghi, M., Khonakdar, H.A., 2016. New  
1116 ternary PLA/organoclay-hydrogel nanocomposites: Design, preparation and study on  
1117 thermal, combustion and mechanical properties. *Mater. Des.* 110, 811–820.  
1118 <https://doi.org/10.1016/j.matdes.2016.08.059>
- 1119 Shao, L., Shi, L., Li, X., Song, N., Ding, P., 2016. Synergistic effect of BN and graphene  
1120 nanosheets in 3D framework on the enhancement of thermal conductive properties of  
1121 polymeric composites. *Compos. Sci. Technol.* 135, 83–91.  
1122 <https://doi.org/10.1016/j.compscitech.2016.09.013>
- 1123 Shirvanimoghaddam, K., Abolhasani, M.M., Li, Q., Khayyam, H., Naebe, M., 2017. Cheetah  
1124 skin structure: A new approach for carbon-nano-patterning of carbon nanotubes.  
1125 *Compos. Part A Appl. Sci. Manuf.* 95, 304–314.  
1126 <https://doi.org/10.1016/j.compositesa.2017.01.023>
- 1127 Shirvanimoghaddam, K., Abolhasani, M.M., Poliseti, B., Naebe, M., 2018. Periodical  
1128 patterning of a fully tailored nanocarbon on CNT for fabrication of thermoplastic  
1129 composites. *Compos. Part A Appl. Sci. Manuf.* 107, 304–314.  
1130 <https://doi.org/10.1016/j.compositesa.2018.01.015>
- 1131 Silva, B.L., Nack, F.C., Lepienski, C.M., Coelho, L.A.F., Becker, D., 2014. Influence of  
1132 intercalation methods in properties of Clay and carbon nanotube and high density  
1133 polyethylene nanocomposites. *Mater. Res.* 17, 1628–1636. <https://doi.org/10.1590/1516-1439.303714>
- 1135 Singla, R.K., Zafar, M.T., Maiti, S.N., Ghosh, A.K., 2017. Physical blends of PLA with high  
1136 vinyl acetate containing EVA and their rheological, thermo-mechanical and  
1137 morphological responses. *Polym. Test.* 63, 398–406.  
1138 <https://doi.org/10.1016/j.polymertesting.2017.08.042>
- 1139 Stern, N., Dyamant, I., Shemer, E., Hu, X., Marom, G., 2018. Hybrid effects in the fracture

1140 toughness of polyvinyl butyral-based nanocomposites. *Nanocomposites* 4, 1–9.  
1141 <https://doi.org/10.1080/20550324.2018.1447827>

1142 Surendran, A., Pionteck, J., Vogel, R., Kalarikkal, N., Geethamma, V.G., Thomas, S., 2018.  
1143 Effect of organically modified clay on the morphology, rheology and viscoelasticity of  
1144 epoxy-thermoplastic nanocomposites. *Polym. Test.* 70, 18–29.  
1145 <https://doi.org/https://doi.org/10.1016/j.polymertesting.2018.06.023>

1146 Szeluga, U., Kumanek, B., Trzebicka, B., 2015. Synergy in hybrid polymer/nanocarbon  
1147 composites. A review. *Compos. Part A Appl. Sci. Manuf.* 73, 204–231.  
1148 <https://doi.org/10.1016/j.compositesa.2015.02.021>

1149 Terzopoulou, Z., Bikiaris, D.N., Triantafyllidis, K.S., Potsi, G., Gournis, D., Papageorgiou,  
1150 G.Z., Rudolf, P., 2016. Mechanical, thermal and decomposition behaviour of poly( $\epsilon$ -  
1151 caprolactone) nanocomposites with clay-supported carbon nanotube hybrids.  
1152 *Thermochim. Acta* 642, 67–80. <https://doi.org/10.1016/j.tca.2016.09.001>

1153 Tjong, S.C., 2014. Synthesis and Structural-Mechanical Property Characteristics of  
1154 Graphene-Polymer Nanocomposites, in: Tjong, S. C. (Ed.), *Nanocrystalline Materials:  
1155 Their Synthesis-Structure-Property Relationships and Applications*. Elsevier,  
1156 Amsterdam, pp. 335–375. <https://doi.org/10.1016/B978-0-12-407796-6.00010-5>

1157 Tsai, T.Y., Naveen, B., Shiu, W.C., Lu, S.W., 2014. An advanced preparation and  
1158 characterization of the PET/MgAl-LDH nanocomposites. *RSC Adv.* 4, 25683–25691.  
1159 <https://doi.org/10.1039/c4ra03171g>

1160 Usuki, A., Yoshitsugu, K., Masaya, K., Akane, O., Yoshiaki, F., Toshio, K., Osami, K., 1993.  
1161 Synthesis of Nylon 6-clay hybrid. *J. Mater. Res.* 8, 1179–1184.  
1162 <https://doi.org/10.1557/JMR.1993.1179>

1163 Venkategowda, C., Rajanna, S., Udupa, N.G.S., Keshavamurthy, R., 2018. Experimental  
1164 investigation of glass- carbon/epoxy hybrid composites subjected to low velocity impact

1165 test. FME Trans. 46, 595–602. <https://doi.org/10.5937/fmet1804595R>

1166 Vyas, M.K., Chandra, A., 2018. Role of organic/inorganic salts and nanofillers in polymer  
1167 nanocomposites: enhanced conduction, rheological, and thermal properties. J. Mater.  
1168 Sci. 53, 4987–5003. <https://doi.org/10.1007/s10853-017-1912-x>

1169 Wang, J.Y., Yang, S.Y., Huang, Y.L., Tien, H.W., Chin, W.K., Ma, C.C.M., 2011.  
1170 Preparation and properties of graphene oxide/polyimide composite films with low  
1171 dielectric constant and ultrahigh strength via in situ polymerization. J. Mater. Chem. 21,  
1172 13569–13575. <https://doi.org/10.1039/c1jm11766a>

1173 Wang, S., Gao, R., Zhou, K., 2019. The influence of cerium dioxide functionalized reduced  
1174 graphene oxide on reducing fire hazards of thermoplastic polyurethane nanocomposites.  
1175 J. Colloid Interface Sci. 536, 127–134.  
1176 <https://doi.org/https://doi.org/10.1016/j.jcis.2018.10.052>

1177 Wani, T.P., Rajab, R., Sampathkumaran, P., Seetharamu, S., 2018. Investigation on Wear and  
1178 Friction Characteristics of Bi-Directional Silk Fibre Reinforced Nanoclay Added HDPE  
1179 Composites. Mater. Today Proc. 5, 25713–25719.  
1180 <https://doi.org/https://doi.org/10.1016/j.matpr.2018.11.013>

1181 Wu, Z., Wang, H., Zheng, K., Xue, M., Cui, P., Tian, X., 2012. Incorporating strong polarity  
1182 minerals of tourmaline with carbon nanotubes to improve the electrical and  
1183 electromagnetic interference shielding properties. J. Phys. Chem. C 116, 12814–12818.  
1184 <https://doi.org/10.1021/jp2121164>

1185 Xiao, Y., Wang, W. yan, Chen, X. jia, Lin, T., Zhang, Y. tong, Yang, J. hui, Wang, Y., Zhou,  
1186 Z. wan, 2016. Hybrid network structure and thermal conductive properties in  
1187 poly(vinylidene fluoride) composites based on carbon nanotubes and graphene  
1188 nanoplatelets. Compos. Part A Appl. Sci. Manuf. 90, 614–625.  
1189 <https://doi.org/10.1016/j.compositesa.2016.08.029>

1190 Xu, Z., Gao, C., 2010. In situ polymerization approach to graphene-reinforced nylon-6  
1191 composites. *Macromolecules* 43, 6716–6723. <https://doi.org/10.1021/ma1009337>

1192 Yang, S.Y., Lin, W.N., Huang, Y.L., Tien, H.W., Wang, J.Y., Ma, C.C.M., Li, S.M., Wang,  
1193 Y.S., 2011. Synergetic effects of graphene platelets and carbon nanotubes on the  
1194 mechanical and thermal properties of epoxy composites. *Carbon N. Y.* 49, 793–803.  
1195 <https://doi.org/10.1016/j.carbon.2010.10.014>

1196 Yuan, B., Fan, A., Yang, M., Chen, X., Hu, Y., Bao, C., Jiang, S., Niu, Y., Zhang, Y., He, S.,  
1197 Dai, H., 2017. The effects of graphene on the flammability and fire behaviour of  
1198 intumescent flame retardant polypropylene composites at different flame scenarios,  
1199 *Polymer Degradation and Stability*. Elsevier Ltd.  
1200 <https://doi.org/10.1016/j.polymdegradstab.2017.06.015>

1201 Yuan, B., Sun, Y., Chen, X., Shi, Y., Dai, H., He, S., 2018. Poorly-/well-dispersed graphene:  
1202 Abnormal influence on flammability and fire behaviour of intumescent flame retardant.  
1203 *Compos. Part A Appl. Sci. Manuf.* 109, 345–354.  
1204 <https://doi.org/10.1016/j.compositesa.2018.03.022>

1205 Yue, L., Pircheraghi, G., Monemian, S.A., Manas-Zloczower, I., 2014. Epoxy composites  
1206 with carbon nanotubes and graphene nanoplatelets - Dispersion and synergy effects.  
1207 *Carbon N. Y.* 78, 268–278. <https://doi.org/10.1016/j.carbon.2014.07.003>

1208 Zaferani, S.H., 2018. Introduction of polymer-based nanocomposites, in: Jawaid, M., Khan,  
1209 M. (Eds.), *Polymer-Based Nanocomposites for Energy and Environmental Applications*.  
1210 Woodhead Publishing, Elsevier, pp. 1–25. [https://doi.org/10.1016/B978-0-08-102262-](https://doi.org/10.1016/B978-0-08-102262-7.00001-5)  
1211 [7.00001-5](https://doi.org/10.1016/B978-0-08-102262-7.00001-5)

1212 Zhang, H., Zhang, G., Tang, M., Zhou, L., Li, J., Fan, X., Shi, X., Qin, J., 2018. Synergistic  
1213 effect of carbon nanotube and graphene nanoplates on the mechanical, electrical and  
1214 electromagnetic interference shielding properties of polymer composites and polymer

1215 composite foams. *Chem. Eng. J.* 353, 381–393. <https://doi.org/10.1016/j.cej.2018.07.144>

1216 Zhang, W.-D., Phang, I.Y., Liu, T., 2006. Growth of Carbon Nanotubes on Clay: Unique  
1217 Nanostructured Filler for High-Performance Polymer Nanocomposites. *Adv. Mater.* 18,  
1218 73–77. <https://doi.org/10.1002/adma.200501217>

1219 Zhao, B., Wang, S., Zhao, C., Li, R., Hamidinejad, S.M., Kazemi, Y., Park, C.B., 2018.  
1220 Synergism between carbon materials and Ni chains in flexible poly(vinylidene fluoride)  
1221 composite films with high heat dissipation to improve electromagnetic shielding  
1222 properties. *Carbon N. Y.* 127, 469–478. <https://doi.org/10.1016/j.carbon.2017.11.032>

1223 Zhao, Y.-Q., Lau, K.-T., Wang, Z., Wang, Z.-C., Cheung, H.-Y., Yang, Z., Li, H.-L., 2009.  
1224 Fabrication and Properties of Clay-Supported Carbon Nanotube/Poly (vinyl alcohol)  
1225 Nanocomposites. *Polym. Compos.* 30, 702–707. <https://doi.org/10.1002/pc.20698>

1226 Zhou, E., Xi, J., Guo, Y., Liu, Y., Xu, Z., Peng, L., Gao, W., Ying, J., Chen, Z., Gao, C.,  
1227 2018. Synergistic effect of graphene and carbon nanotube for high-performance  
1228 electromagnetic interference shielding films. *Carbon N. Y.* 133, 316–322.  
1229 <https://doi.org/10.1016/j.carbon.2018.03.023>

1230 Zhu, T., Qian, C., Zheng, W., Bei, R., Liu, S., Chi, Z., Chen, X., Zhang, Y., Xu, J., 2018.  
1231 Modified halloysite nanotube filled polyimide composites for film capacitors: High  
1232 dielectric constant, low dielectric loss and excellent heat resistance. *RSC Adv.* 8, 10522–  
1233 10531. <https://doi.org/10.1039/c8ra01373j>

1234 Zhu, T.T., Zhou, C.H., Kabwe, F.B., Wu, Q.Q., Li, C.S., Zhang, J.R., 2019. Exfoliation of  
1235 montmorillonite and related properties of clay/polymer nanocomposites. *Appl. Clay Sci.*  
1236 169, 48–66. <https://doi.org/https://doi.org/10.1016/j.clay.2018.12.006>

**Graphical abstract:**

